Ca' Foscari University of Venice

Master's Degree program in Environmental Sciences

Final Thesis

Biomarker Record from Lake Fucino (Abruzzo) during MIS-5 for Paleoclimate Reconstructions

Supervisor
Prof. Dario Battistel

Assistant supervisor
Dr. Elena Argiriadis

Graduand
Evans Osayuki Erhenhi

Matriculation Number 860427

Academic Year
2016 / 2017

Contents

1. INTRODUCTION ..... 5~~4~~
1.1. The Earth's Climate System ..... 5~~4~~
1.2. Lake sediments as a climate archive ..... 6~~5~~
1.3. Fire in the Earth system 7
1.4. Biomarker proxies in lake sediments ..... 8~~7~~
1.4.1. Advantages of the biomarker multi-proxy method ..... 9~~8~~
1.4.2. Combustion proxies 10
1.4.3. Proxies for determination of vegetation distribution 15
1.5. Challenges in using lake sediments as climate archive 16
1.6. Study Area 16
1.7. Objective 17
2. METHODS AND INSTRUMENTATION 18
2.1. Materials and instrument 18
2.1.1. Accelerated solvent extraction 18
2.1.2. Turbovap 19
2.1.3. Gas-Chromatography and Mass -Spectrometry (GC-MS) 19
2.1.4. Ion-Chromatography and Mass -Spectrometry (IC-MS) 20
2.2. Methods 21
2.2.1. Age-Depth model 21
2.2.2. Sample preparation 22
2.2.3. Sample extraction 23
2.2.4. Sample concentration and volume reduction 24
2.2.6. Derivatization 25
2.3. Quantification 25
2.3.1. n-Alkanes analysis 25
2.3.2. Polycyclic Aromatic Hydrocarbons 25
2..3.4. Monosaccharide anhydrides 27
Fig.2.8. Diagram showing methods procedures. 28
3. RESULTS ..... 29~~28~~
3. DISCUSSION ..... 35~~34~~
4.1 Vegetation Distribution 35
4.1.2. Long chain n-alkanes (LCH > C_{23}) 35
4.1.2. Terrigenous/aquatic ratio (TAR) 36
4.5. Comparison of the proxies 38

2. CONCLUSION 41
Reference 42
Appendix 51

1. INTRODUCTION

1.1. The Earth's Climate System

The Earth is a dynamic system where all its components are constantly changing. The changes in the Earth's components are intertwined with the Earth's climate system. Thus, changes in the biosphere, geosphere, and hydrosphere can lead to climate changes and, in return, these components can be affected by the changes in Earth's climate. However, variation in the Earth's climate has had a considerable impact on society on a different scale, throughout human history, such as water resource, agriculture, fisheries recreation. Humans have been said to be responsible for the trend of climate warming in the past decades, but attention must be given to understanding and quantifying the variability of these changes for solution purpose (Lazier, 1995; IPCC Climate Change, 2007; Masson-Delmotte *et al.*, 2015), it is difficult for scientists to make future projections about climate change, because of the complexity of Earth`s climate system. Although models for climate simulation are being created and constantly improving, models have uncertainty in projections since they are simulations (Bruckner, 2017). In order to be able to make an educated and well-informed scientific projection about the future, it is important to understand in full richness the dynamics of Earth`s climate variations, how and why climate have changed over time throughout Earth's history, how plant and animal populations responded to the changes. This can be done by assessing climate sensitivity to different factors, and the knowledge can be used as a baseline study for long-term variability and response to variations in climate change (Li, Nychka and Ammann, 2010; Monica Bruckner, 2017).

Information revealing past climate conditions are stored in environmental record known as climate archives, formed through any environmental process that has accumulated over time in layers, such as ice cores, tree rings, marine and lake sediments. The parameters that are analyzed in these archives are known as proxies, which are any piece of evidence that can be used to infer past climate condition (Lazier, 1995; Amann *et al* 2014). A lot of information about the past climate can be revealed through these archives at different resolution, from local to global scale: using climate archives to reconstruct past environment gives an insight of climate conditions.

1.2. Lake sediments as a climate archive

Lakes are water bodies often recharged from surface runoff, groundwater, and precipitation. They may be shallow or deep, permanent or temporary, be created artificially by humans or occur naturally as a result of glacial, erosional, fluvial or volcanic activity. It is possible for a lake to dry out naturally or be drained by humans: a dried-out lake with sediment left behind is known as lacustrine plain (Nelson and Fussmann, 2002).

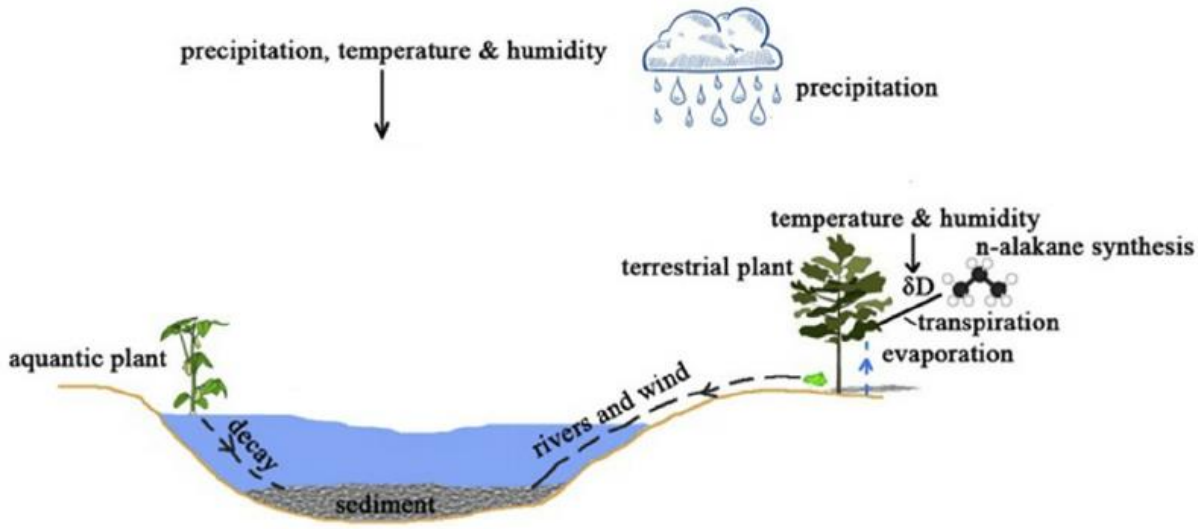

Fig.1.1. Sedimentation process in Lake (Ouyang, Guo and Bu, 2015).

The study of lakes is known as limnology, while paleolimnology is referred to the study of past lake and catchment changes inferred from sediments. As the lake is formed, it begins to store information about the environment through the deposition of sediments that accumulate in successive layers over time. Each layer has different and unique information about the environmental condition at the time the sediment was deposited, from the ecosystem level to climatic conditions, such as human activities and organism that lived in the environment, soil types, vegetation distribution, fire events and the contribution of humans that lived in the environments. This information is gathered from the materials of the environment that have been transported into the lake through surface runoff, wind transportation, erosion and organisms from the lake. The components of sediment are often typically categorized, usually on a broad level, by the origin in which they are deposited into the lake. There are two main

categories: (*i*) allochthonous components are sediment depositions which are transported from outside the lake, such as soil, pollen grains, and atmospheric depositions; (*ii*) autochthonous components originate from within the lake, including aquatic vertebrates and particles such as algae (Cañellas-Boltà *et al.*, 2012). These materials are deposited at the bottom of the lake within sediments and hold information about the past. Scientists started taking steps in quantifying the information stored in lake sediment cores in the early 1980s, this practice has grown over the past years being that a lot of proxies can be analyzed in lake sediment (Last and Smol, 2002). Lake sediments cores have materials that are useful for examining and understanding the link between climate variables, and how this relationship may affect climate fluctuation from local to regional scale (Kehrwald *et al.*, 2010).

1.3. Fire in the Earth system

Although humans have an inseparable relationship with fire, which they have been using for a very long time, since the introduction of agriculture to clear the landscape. However, wildfire has been a part of natural system for millions of years, since terrestrial plants appear. Fire events release aerosols and greenhouse gases, such as carbon dioxide and methane, which influence climate at a global scale, and the changes in climatic conditions such as temperature and level of moisture in turn have a huge control on fire occurrence and the probability for fire to spread. It is very difficult to separate anthropogenic contribution from natural cause of fire event in the Holocene because the use of fire by early humans may have had impact on the climate variability as we have seen in recent years with the warming of Earth's climate, which is directly connected to the emission of carbon dioxide through human activities. Some studies have been able to correlate the appearance of humans with local fire events, major vegetation changes and climate cycle, suggesting that humans may have played a part in shaping the Earth`s climate thousands of years ago, through the emission of methane and carbon dioxide from fire events such as biomass burning in relationship with the beginning of agriculture. Studies have also shown that there were seasonal wildfire, long before human started using fire (Kehrwald *et al.*, 2010; Schüpbach *et al.*, 2015).

1.4. Biomarker proxies in lake sediments

The sediment proxies discussed in this section are the molecular markers considered for this research. Biomarkers are organic compounds which have conserved their structure and also have a recognizable source (Ball, 1996). In this regard, a good tracer should, therefore, be source-specific and stable in the environment. Biomarkers stored in lake sediments are investigated in several ways, and are useful for the reconstruction of past environmental conditions, such as temperatures, precipitation, vegetation distribution, and how they will react to different stressors such as climate change, nutrient enhancement or atmospheric pollution and other conditions in qualitative or quantitative ways (Last and Smol, 2002; Cañellas-Boltà *et al.*, 2012). Among the numerous proxies in lake sediments, three classes of molecules are employed and discussed in this research. (1) *n*-Alkanes are used as vegetation distribution indicators: when the vegetation composition is known, it is easy to decipher the climatic conditions that support the vegetation type. (2) Polycyclic aromatic hydrocarbons and (3) monosaccharide anhydrides (levoglucosan, mannosan and galactosan), are used as indicators of fire activities, allowing the correlation between fire and vegetation (D'Anjou *et al.*, 2012).

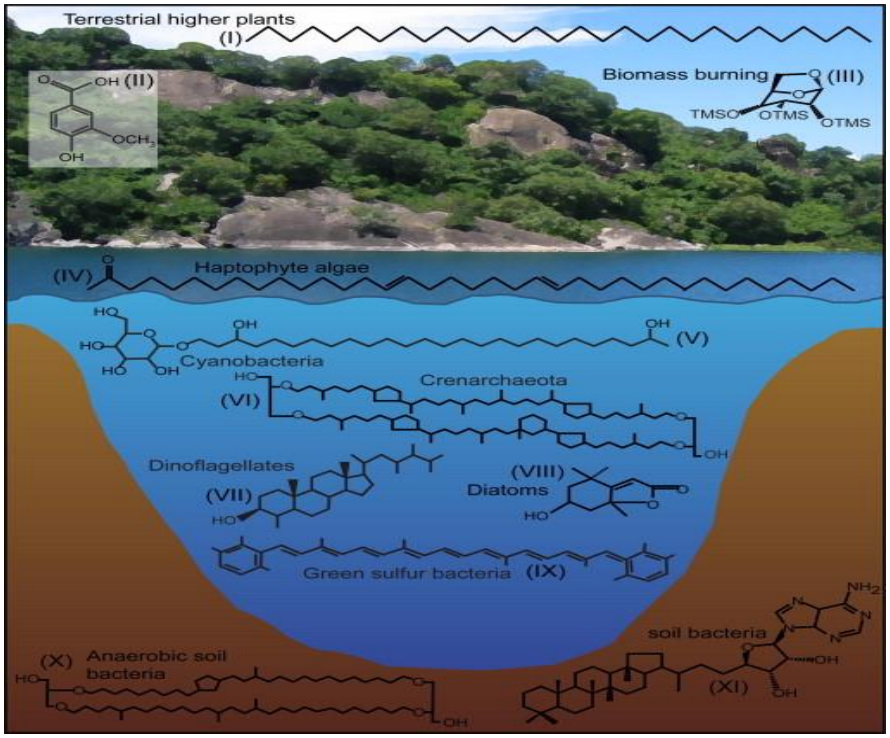

Fig.1.2. Organic matter decomposition process in lake sediment. Higher land plants, different algae, microbes living in the soil and microorganisms that live in the water column (Castañeda and Schouten, 2011).

1.4.1. Advantages of the biomarker multi-proxy method

Climate proxies in lake sediments are of different types and are generated from different sources, they have different deposition processes and they are sensitive to climate variability in different ways, therefore preserve climate information differently. One tracer might be good at short time scale, while another better at a longer time scale, with each giving different environmental and climatic information (Li, Nychka and Ammann, 2010). Combining different biomarker in sediments can give a complete information about past environmental condition when done properly (Kehrwald *et al.*, 2010). Paleoenvironmental reconstruction based on multi-proxy studies typically provides much stronger environmental and ecological understanding: lake deposits are a perfect archive for multi-proxy analysis, because their organic content provides different types of proxies that are significant to the explanation and clarification of both natural and human-induced changes (Last and Smol, 2002; Cañellas-Boltà *et al.*, 2012).

n-Alkanes: Indicator for vegetation distribution

Monosaccharide Anhydrides (MAs) and Polycyclic Aromatic Hydrocarbon (PAHs): Indicator for Biomass burning (wildfire)

Fig.1.3. Biomarkers considered in this research.

1.4.2. Combustion proxies

Fire is a worldwide phenomenon which appears in the environmental record soon after terrestrial plants appearance. Proxies that indicate biomass burning in lake sediment are useful for reconstructing the relationship between climate and fire activities. Understanding wildfire and biomass burning is a significant factor in the context of climate change because fires directly affect global carbon storage, ecosystem processes and patterns and atmospheric chemistry, including vegetation structure and distribution (Denis *et al.*, 2012). The knowledge of the natural mechanisms that control fire occurrence in ecosystems requires a continuous record that can be obtained from the reconstruction of past fire events (Bowman 2009, Denis et al. 2012). Fire influences climate by the emission of aerosols into the atmosphere, which acts as condensation nuclei, blocking the sun reflection and also prevent the escape of heat from the troposphere (Jimenez, Canagaratna and Worsnop, 2009; Kehrwald *et al.*, 2010). Since fire frequency and intensity are influenced by climate conditions, tracers of fire events are often used to deduce and reconstruct what the climate was like in the past. The vegetation composition, directly related to local and regional temperature and humidity, determines fuel conditions and fire dynamics. Fuel chemical composition and the temperature and time of combustion determine the type of molecular alteration and transformation of the organic compounds emitted during biomass combustion (Simoneit, 2002; Khedidji *et al.*, 2017).

Polycyclic aromatic hydrocarbons (PAHs) produced during wildfires usually record the fire events at a local to regional scale, since they are subject to atmospheric transport. Levoglucosan is used as a specific molecular marker for biomass burning, as it can only be produced through combustion of cellulose at a temperature greater than 300 $^{\circ}$C and is present in lake cores as a result of atmospheric deposition (Kehrwald *et al.*, 2010; Denis *et al.*, 2012).

- **Monosaccharide anhydrides (MAs)**

  Monosaccharide anhydrides are among the most important compounds used for the reconstruction of biomass burning, in particular, levoglucosan (1,6-

anhydro-β-D-glucopyranose) and its isomers galactosan (1,6- anhydro-β-D-galactopyranose) and mannosan (1,6-anhydro-β-D-mannopyranose) (Kehrwald *et al.*, 2010; Fraser and Lakshmanan, 2000; Jordan, Seen and Jacobsen, 2006).

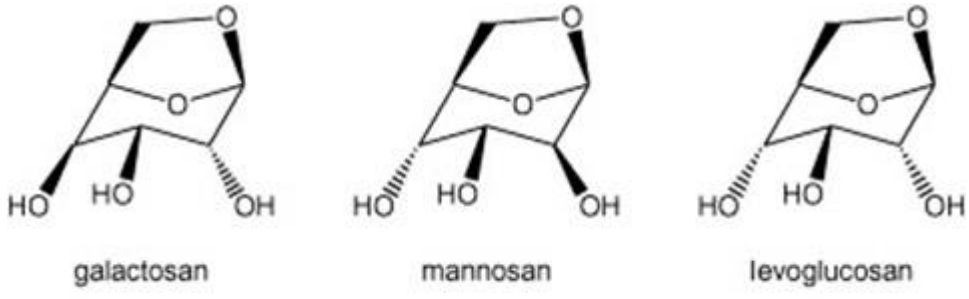

Fig 1.4. Chemical structure of galactosan mannosan and levoglucosan (Hsu *et al.*, 2007).

MAs are commonly used as an atmospheric molecular tracer for the biomass burning which can only be produced by burning plant tissue. Among MAs, levoglucosan has been disclosed to be a good target because it is released in very high amounts and it also has high resistance to degradation, it can be detected at significant distance from the combustion source (Simoneit *et al.*, 1999; Jordan, Seen and Jacobsen, 2006). The emission factor of levoglucosan from biomass burning has been shown to be usually very high, suggesting it as a good tracer for this process (Natalie Kehrwald et al. 2010; Simoneit et al. 1999).

Table 1.1. The composition and source of MAs (Simoneit, 2002).

Compound	**Composition**	**Indicator For source**
Levoglucosan	$C_6H_{10}O_5$	Cellulose
Mannosan	$C_6H_{10}O_5$	Hemicellulose
Galactosan	$C_6H_{10}O_5$	Hemicellulose

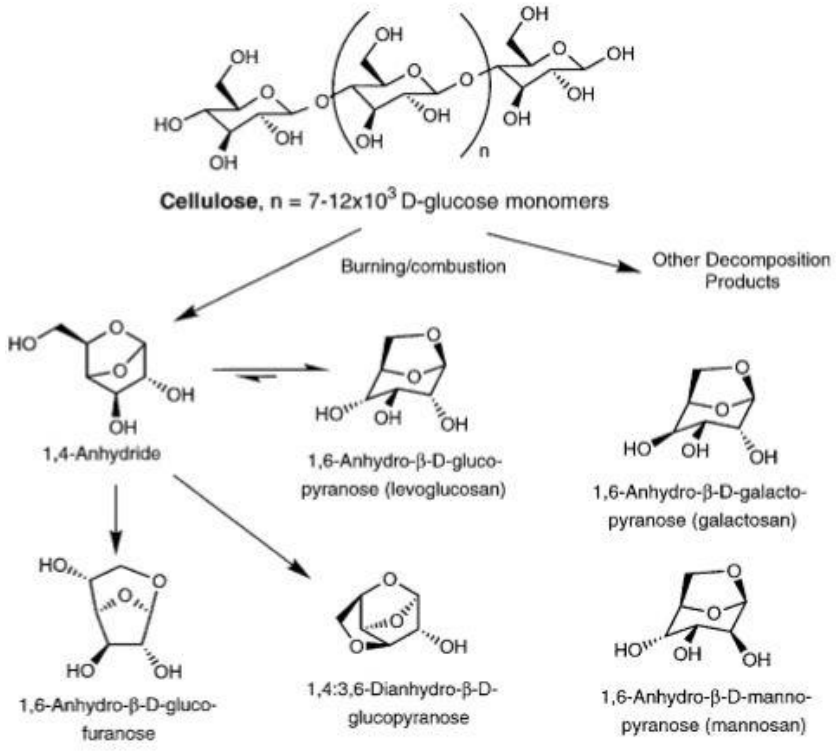

Fig 1.5. Degradation process of cellulose to form levoglucosan galactosan and mannosan, the three MAs are formed through similar processes: mannosan and galactosan are formed through hemicelluloses (Simoneit, 2002).

- **Polycyclic aromatic hydrocarbons (PAH)**

Polycyclic aromatic hydrocarbons (PAHs) are organic compounds categorized by the occurrence of aromatic rings fused together, between two and six or more rings. PAHs may be synthesized from saturated hydrocarbons under oxygen deficient conditions (WHO, 2000). The major processes which explain PAHs formation are pyrosynthesis and pyrolysis. (Ravindra, Sokhi and Van Grieken, 2008). They are produced during the incomplete combustion of organic materials, including forest vegetation during wildfires or burning of fossil fuel, most especially through human actions such as the incomplete combustion of organic materials through industrial activity, combustion of wood for the purpose of energy production, coal and processing of crude oil, combustion of refuse and smoking of tobacco, as well as natural processes such as carbonization (WHO, 2000). 3–6 ring PAHs are mostly predominantly unbranched. Forest fires increase the pyrogenic PAHs concentration in the atmosphere and eventually in sediments: this makes pyrogenic PAHs distinguishable from petrogenic PAHs, which often

have a branched or substituted structure and are petroleum based (Denis *et al.*, 2012). There are several hundred PAHs, the best known is benzo[*a*]pyrene (BaP) and a lot of information on the toxicity and incidence of PAHs is linked to BaP. PAHs are connected with human health hazardous effects (Richter *et al.*, 2000; WHO, 2000), they are extensively circulated in the troposphere and are one of the foremost atmospheric pollutants (Ravindra, Sokhi and Van Grieken, 2008). It has also been proven that PAHs can cause carcinogenic effects and they are formidable immune suppressants. Effects have been recognized on immune system development, human immunity and on host resistance, the process of toxicity is thought to be interfering with the function of cellular membranes as well as with enzyme systems which are associated with the membrane (Abdel-Shafy and Mansour, 2015). Carcinogenicity of PAHs increases with molecular weight (Ravindra, Sokhi and Van Grieken, 2008).

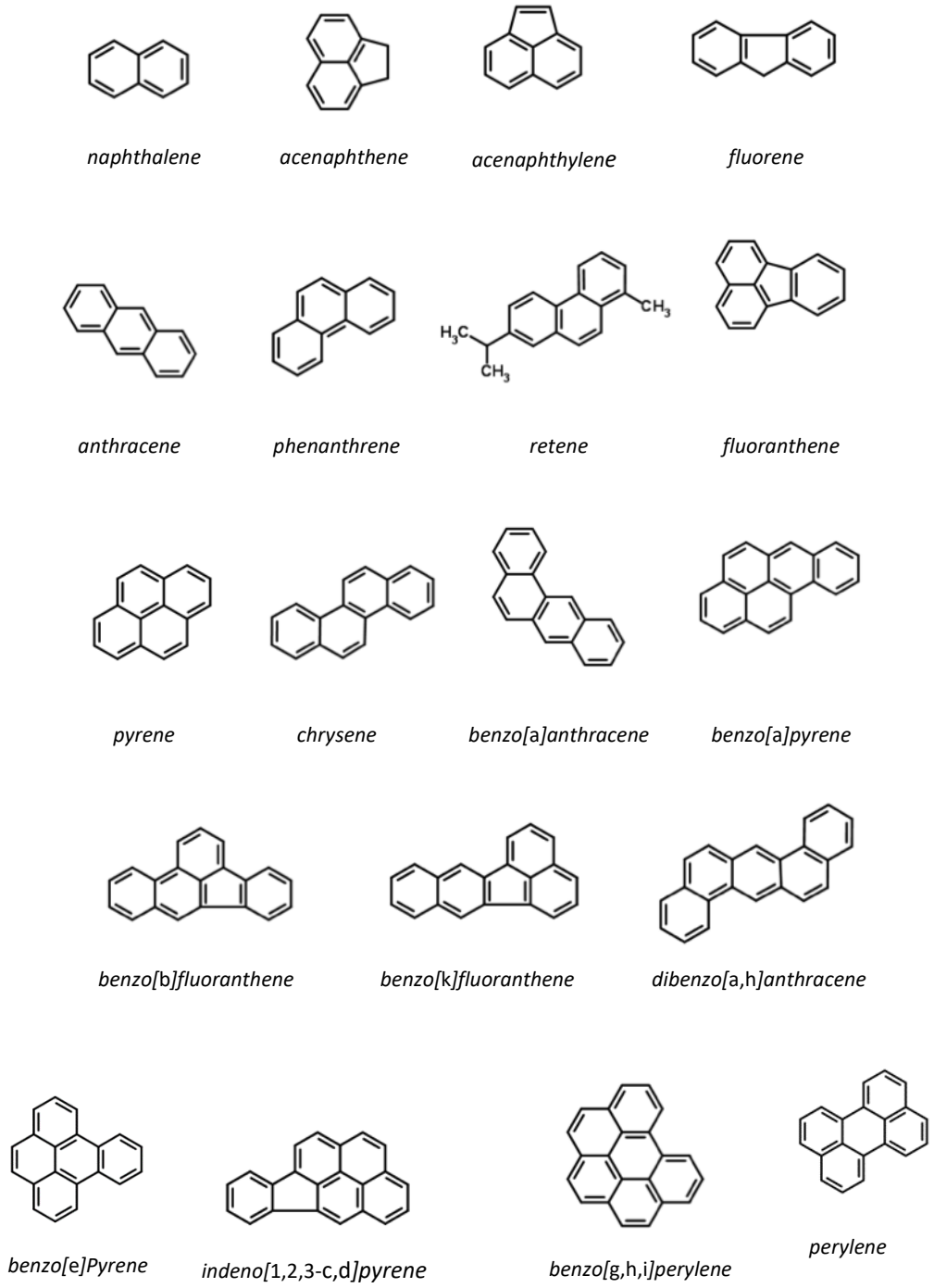

Fig:1.6. Chemical structure of PAHs analyzed in this research (Pampanin and Sydnes, 2013).

Since the main source is combustion, PAHs in sediments are used as proxies for the rate of recurrence and proportions of forest fires, connected to both past environmental conditions and human activities for the reconstruction of the historical record in pre-industrial periods

(Musa Bandowe *et al.*, 2014). PAHs adsorbed to particles in the atmosphere can be transported and reach the surface of lakes, streams, and oceans through wet and dry deposition. Eventually, such particles sink to the sediment, similarly to the processes in which surface soil is deposited (Baek *et al.*, 1991).

PAHs deposited in lakes have some characteristics that make them attractive fire indicators, such as their resistance to degradation and the production within a broader temperature range than charcoal (PAHs: 200–900 ºC or higher, charcoal: 200–600 ºC). This allows reconstructing higher temperature events compared to charcoal (Denis *et al.*, 2012). Moreover, individual PAH distribution can provide information about the type of material that was combusted: different kinds of fuels result in different burning conditions and thus produce different PAH patterns (Jenkins *et al.*, 1996; Denis *et al.*, 2012; Yang, Lin and Chang, 2007; Jimenez *et al.*, 2017).

1.4.3. Proxies for determination of vegetation distribution

n-Alkanes (NA)

n-Alkanes are produced from the wax coats on plant leaves and other plant organs, including lower plant groups. there are quantitative variations in the pattern of *n*-alkane from plant to plant, but the pattern is generally similar. Their distribution is sensitive to environmental conditions and they are imperative in the reconstruction of paleoenvironmental vegetation distribution. Long-chain *n*-alkanes result from leaf waxes, it is an indication of terrigenous input and reflects the composition of vegetation. The distribution of *n*-alkanes in the leaves of vascular plants is related to the environmental condition or changes in the environment, *n*-alkanes are used as plant biomarkers, because they are relatively resistant both to diagenetic processes and to biochemical degradation in sedimentary records (Zhang *et al.*, 2017; Badejo *et al.*, 2014). *n*-Alkanes are not used to identify plant species, although there can be a big difference in their distribution among different ones. Research has suggested that long chain *n*-alkanes (C26–C33 alkanes) are derived primarily from the leaf wax of higher plants (Badejo *et al.*, 2014).

1.5. Challenges in using lake sediments as climate archive

Using sediment to reconstruct the climate can be challenging because not all components in the lake system are attributed to climatic factors, components such as hydrologic, geomorphology settings and the aging process of a lake may adjust or modify the response of a given climate perturbation. These characteristics that are non-linear and non-stationary may produce incorrect information in the timing of the inferred changes (Fritz, 2008).

1.6. Study Area

Fucino plain is an endorreic basin, located in central Italy with a surface area of 200 km^2 surrounded by carbonate ridges. Historically, the plain was covered by Fucino lake and was in the top three largest Italian lakes. Among the central Italy intermountain tectonic depressions, Fucino lake is amongst the oldest lakes in Italy and the only lake to continuously host lacustrine succession, since the late Plio–Quaternary. Recently it was filled with alluvial and lacustrine deposits, mainly silt and clay with sandy layers, the thickness of the sediments varies in size, it ranges from 100 to 1000 m of primarily silt, with sandy layers, this is due to the main faults reactivation. A channel was built underground in the first century AD to control devastating floods. After preliminary success, the efficiency of channel's speedily declined and the ancient lake water level was restored (Schellekens and Buurman, 2011; Badejo *et al.*, 2014; Zhang *et al.*, 2017). There was draining of Fucino lake toward the end of the nineteenth century (1873). The reason for this is that because of its shallowness, the lake level would change rapidly in response to changes in climatic forcing. These changes in lake level produced considerable damage to the people living on the lake's shores and to the agricultural activities that flourished in the surrounding basin. The major source of replenishment for the lake was autumn and winter rainfall. Precipitation transported erosional debris from the hills that surround the lake, causing the lake water to be muddy and creating a wide area of marsh (Tomassetti *et al.*, 2003).

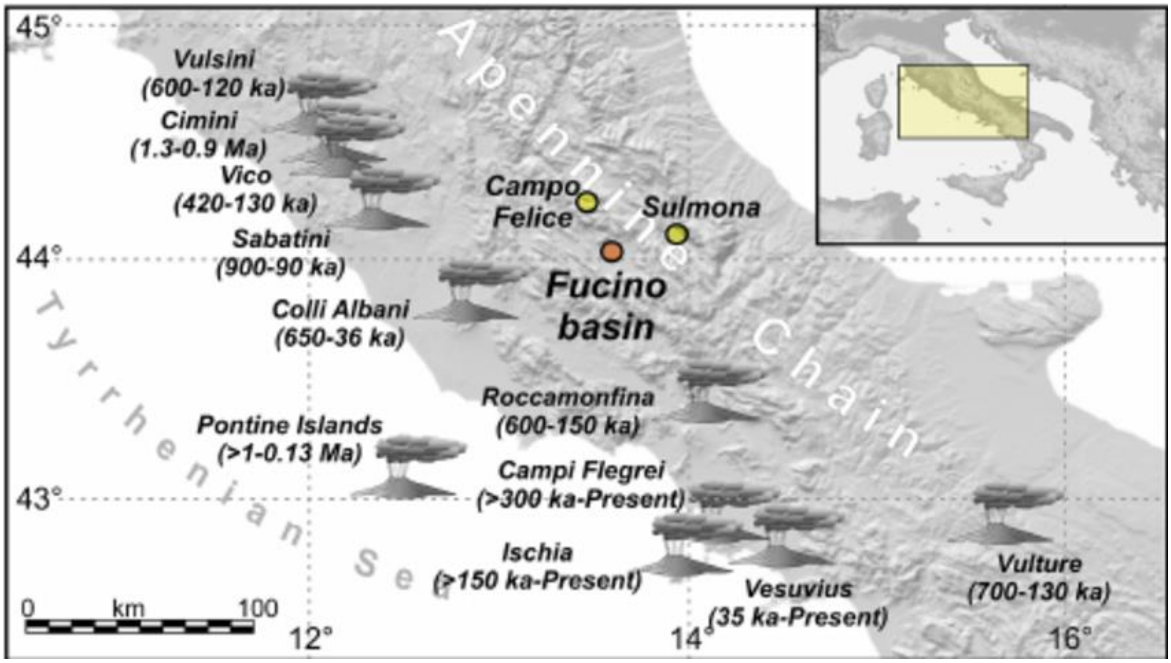

Fig 1.6. Location of the Fucino plain (Giaccio *et al.*, 2015).

1.7. Objective

The marine isotope stage 5 (MIS-5) is significant in paleoclimatological studies due to its abundance and accessible paleoclimate archives, with a profound existence of climate variability under glacial and interglacial boundary conditions, which helps in understanding the dynamics and feedbacks of climate change (Milner *et al.*, 2016). The objective of this research is to understand the relationship between fire and environment in an interglacial period, although from a climatic point of view it resulted slightly different from the present interglacial (Holocene), where human influence can be assumed as negligible. To this purpose, the environmental changes in central Italy during the last interglacial from 60 to 160 kyr before present. will be reconstructed using a multi-proxy approach. 100 samples of lacustrine sediment from Lake Fucino, located in the Abruzzo region (central Italy) will be analyzed for *n*-Alkanes, Polycyclic Aromatic Hydrocarbons (PAHs), and Monosaccharide Anhydrides (MAs – levoglucosan, mannosan, and galactosan) in order to determine fire events and vegetation distribution. This research focuses on the MIS-5, aiming to provide useful insights in the perspective of disentangling natural from anthropogenic contribution in fire dynamics during the Holocene.

2. METHODS AND INSTRUMENTATION

Analytical chemistry was the research tool used for this work, and all the analyses were carried out at the Environmental Analytical Chemistry Laboratory of Ca' Foscari University of Venice.

2.1. Materials and instrument

- 350 Accelerated Solvent Extractor (Dionex Thermo Fisher ASE 350)
- Turbovap® (Caliper Life Science)
- Centrifuge
- Sonic bath
- Ion-Chromatography and Mass-Spectrometry (IC-MS)
- Gas-Chromatography and Mass-Spectrometry (GC-MS)
- SPE tubes

2.1.1. Accelerated solvent extraction

The extraction of solid samples is performed by the accelerated solvent extraction technique. The ASE uses high temperature and pressure to boost the effectiveness of the extraction procedure with organic solvents. Additionally, the extraction kinetics are elevated by increased and elevated temperature and pressure: this guarantees fast and safe extraction by keeping the solvents above boiling point (Thermo Dionex, 2017).

Fig.2.1. 350 Accelerated Solvent Extractor (Thermo Dionex, 2017).

2.1.2. Turbovap

TurboVap II® Concentration Workstation is a microprocessor controlled concentrator that automatically evaporates samples. The concentrator operates with a gas vortex, constantly flowing onto the extracts until the desired volume. Glass concentration tubes are placed in a thermostatic bath: the temperature can be set according to solvent and analyte characteristics, in order to guarantee volume reduction while preventing the evaporation of target compounds (Ab, 2010).

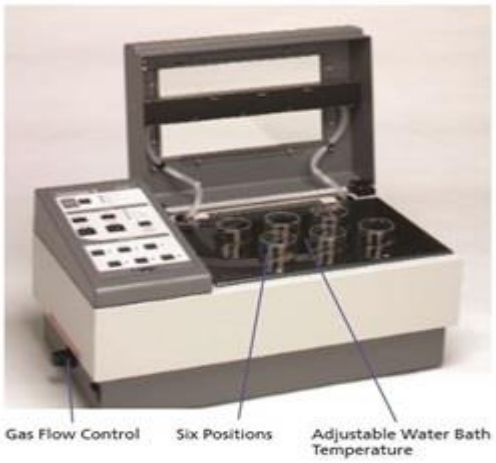

Fig.2.2. TurboVap II. source: TurboVap manual (Ab, 2010)

2.1.3. Gas-Chromatography and Mass -Spectrometry (GC-MS)

Gas chromatography-mass spectrometry (GC-MS) is an analytical technique employing gas chromatography (GC) for the separation of analytes and mass spectrometry (MS) for quantification. GC-MS is used for the analysis of hundreds of different environmental chemical compounds, which are mainly volatile. In this work, an Agilent 7890 GC system coupled to an Agilent 5975 MSD quadrupole mass spectrometer was used, working in positive mode and equipped with an electron impact ion source.

Once injected into the system, the solution is vaporized in the GC inlet, and it is moved by the carrier gas (helium) to the chromatographic column (Agilent HP5-MS capillary column, (5%-phenyl)-methylpolysiloxane, 60 m, 0.25 mm inner diameter, 0.25 μm film thickness), where compounds are separated according to their boiling point as the oven temperature increases. After separation, compounds are transferred into the ion source and analyzed through a single quadrupole. This equipment was used for the analysis of *n*-alkanes and polycyclic aromatic hydrocarbons (Thermo Fisher, 2017).

Fig.2.3. Gas chromatography and mass spectrometry (GC-MS), source. https://www.thermofisher.com (Thermo Fisher, 2017)

2.1.4. Ion-Chromatography and Mass -Spectrometry (IC-MS)

Ion Chromatography-mass Spectrometry (IC-MS), is a technique for the analysis of water-soluble ionic compounds. An ion chromatographic system (Dionex, ICS 5000, Thermo Fisher Scientific) coupled to a single quadrupole mass spectrometer (MSQ Plus, Thermo Fisher Scientific), operating with electrospray ionization in the negative mode, was used. A CarboPacTM PA10 column (ethylvinylbenzene 55% cross-linked with divinylbenzene, 2 x 250 mm, Thermo Fisher Scientific) was employed for the separation together with an AminoTrapTM pre-column (polymeric resin, 2 x 50 mm, Thermo Fisher Scientific). Separation is done when the analyte goes through MA1 column by exchanging ions in the ion chromatography, with the help of sodium hydroxide, the sodium hydroxide is filtered by the suppressor to prevent it from entering the mass spectrometer with the analyte, The MS operates with electrospray ionization in the negative mode, by losing one proton ion. This equipment was used for the analysis of monosaccharide anhydrides ((MAs) levoglucosan, mannosan and galactosan) (Thermo Fisher, 2017).

 s

Fig.2.4. Ion-Chromatography and Mass -Spectrometry (IC-MS) (source: http://iss-store.co.uk).

2.2. Methods

A multiple proxy analysis was conducted for 100 samples of lake sediment core from Lake Fucino. The sediment core was 60 m long, samples were dated with $^{40}Ar/^{39}Ar$ method to be about 180,000 years (Giaccio *et al.*, 2015), and covers the glacial–interglacial cycles from the marine isotope stage 5 (MIS 5). The Fucino sedimentary succession has the advantage to produce a long, independent, continuous and sensitive paleoclimate archive for the central Mediterranean area, as explained by Giaccio et al (2015). The analyses were carried out with GC-MS and IC-MS methods, based on published articles.

2.2.1. Age-Depth model

It is essential to establish the age of sediment core as precisely as possible with absolute or relative dating methods, Although different calibration of the $^{40}Ar/^{39}Ar$ chronometer have been proposed, and are currently in use, the ages that is produced by these different calibrations vary by ~1% , this implies a difference in the calibration of age (Regattieri *et al.*, 2017). The age and dating of the sediment samples used for this research was adopted from the age given by Giaccio et al. (2017) since they have worked with the same samples

previously. $^{40}Ar/^{39}Ar$ method was used for the sample dating, in acquiring the independent age. For the full analytical procedure of the age model, see Giaccio *et al.* (2015 and 2017).

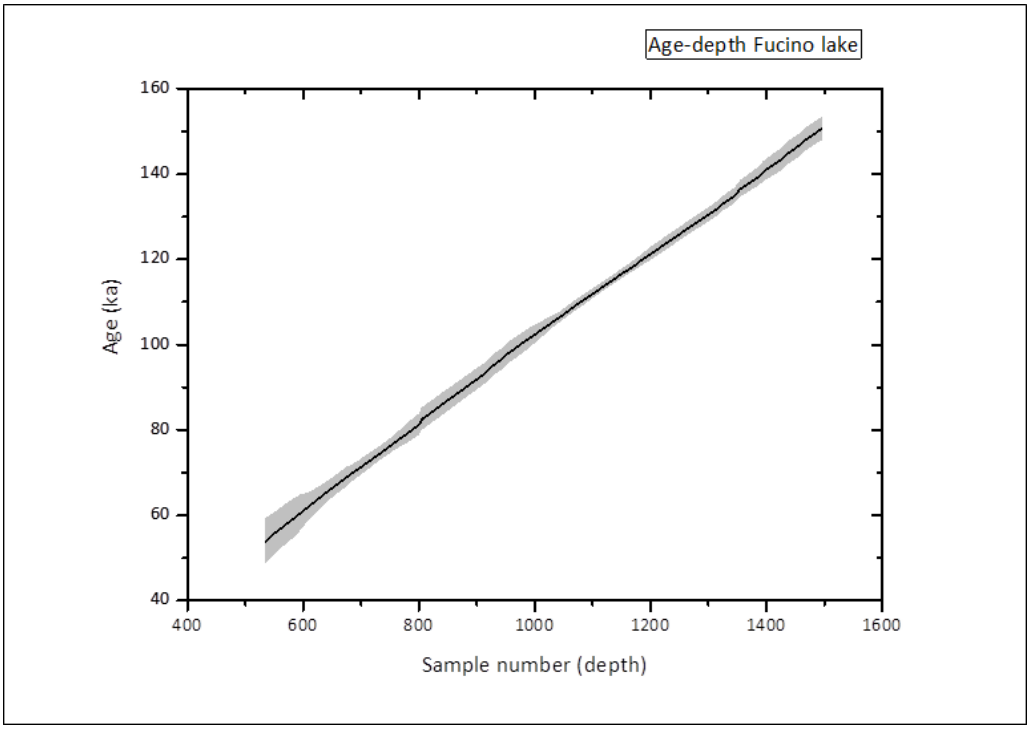

Fig.2.5. Age depth model for the Lake Fucino core (grey area represents the age uncertainty).

2.2.2. Sample preparation

Samples were freeze-dried at the University of Pisa laboratory facilities, then crushed and grinded with ceramic mortar and weighed using a technical scale. Before the extraction was carried out, internal standard solutions were prepared to be used for quantifying different analytes. In this work, ^{13}C-labeled compounds were used as internal standards, by spiking them in known amounts onto samples prior to extraction. Adding the internal standard as early as possible in the procedure is very important, in order to attain the maximum precision (Cavinato *et al.*, 2002; Tomassetti *et al.*, 2003; Lacey *et al.*, 2016).

The internal standard is assumed to undergo the same loss as the analyte during sample preparation and thus is used to quantify the absolute quantity and concentration of the analyte according to the isotope dilution technique, as follows:

$Q = A_n/A_{is} * Q_{is}/RF_n$

where

A_n: area of native compound peak

A_{is}:area of internal standard peakQ_{is}: amount of internal standard

RF_n: response factor for the native compound

For the monosaccharide anhydrides: $A_n/A_{is} = RF * C_n/C_{is}$

Response factors are solutions containing all native compounds and internal standards at the same concentration, analyzed repeatedly together with the samples in order to correct the results according to the instrumental sensitivity towards each specific compound.

$RF = A_n/A_{is} * C_{is}/C_n$

A solution for the internal standard was made for *n*-alkanes, polycyclic aromatic hydrocarbon (PAHs) The internal standard for the monosaccharide anhydrides was created separately, and introduced at a different stage.

- Three internal standards were used for the quantification of PAHs: $^{13}C_6$-Acenaphthylene, $^{13}C_6$-Phenantrene, and $^{13}C_4$-Benzo(*a*)pyrene (1 pg μL^{-1});
- Hexatriacontane (C_{36}) was used as internal standard for *n*-alkanes (50 ng μL^{-1})
- ^{13}C-Cholesterol was used as the internal standard for the fecal and plants sterols (2 ng μL^{-1});
- ^{13}C-levoglucosan was used as an internal standard for the MAs (1 ng μL^{-1}).

2.2.3. Sample extraction

Sample extraction was carried out as explained in Battistel et al. (2015) with little modifications. Extraction was done with a Dionex Thermo Fisher ASE 350 (Accelerated Solvent Extractor) with 20 mL stainless steel extraction cells. The extraction cells were prepared by first placing 5n mm of diatomaceous earth at the bottom of the cell, before adding the samples, which were then spiked with 50 µL internal standard solution for NA, PAHs and FPS, anhydrous sodium sulfate (Na_2SO_4) was added to the cells to eliminate any

trace of water/moisture, the cells were filled with diatomaceous earth, then sealed and shook for proper mixture of the elements. The samples were extracted with 3 extraction cycles (static: 5 min) at 100 °C and 1500 psi, using dichloromethane (DCM) for the first two cycles (E_{1+2}) and methanol (MeOH) for the third cycle (E_3). Extracts from the third cycle were collected separately and spiked with 100 µL of the $_{13}$C-levoglucosan solution. E_{1+2} was used for the analysis of *n*-alkanes, PAHs and the fecal and plant sterols, E_3 was used for the MAs (levoglucosan, mannosan, and galactosan). The samples extracted were kept in the refrigerator, for the next step of the analysis.

2.2.4. Sample concentration and volume reduction

DCM extracts were placed in the Turbovap at 23 ºC and evaporated to 0.5 mL under a gentle stream of nitrogen. The MeOH extracts were concentrated as explained by Kirchgeorg, et al. 2014 and Schüpbach et al. 2015: they were placed in the TurboVap at 35 ºC, until complete dryness. Samples were redissolved in 500 µL of ultra-pure water then placed in the ultrasonic bath for 10 minutes, to avoid any adsorption to the walls of the evaporation glass.Finally, samples were transferred to centrifuge for 10 minutes at 14,000 rpm, after which they were transferred to IC-MS measurement vials (Kirchgeorg *et al.*, 2014; Schüpbach *et al.*, 2015).

2.2.5. Sample cleanup and second reduction

The cleanup, derivatization and the GC-MS method was carried out as explained in Battistel et al. 2015. The E_{1+2} samples were further separated into two fractions during the cleanup process, fraction 1 (F1) and fraction 2 (F2). F1 was used for the analysis of *n*-alkanes and PAHs while F2 was used for the analysis of fecal and plant sterols. The clean-up was based on solid phase extraction method (SPE) with disposable neutral silica tubes (Supelco DSC...), topped with aluminum oxide, then conditioned with 40 mL of n-hexane:dichloromethane = 1:1 until the stationary phase appeared to be homogeneous and translucent, then

samples were loaded onto the SPE tubes. F1 was eluted with 15 mL of HEX:DCM=1:1. The F2 was eluted with 100 mL DCM. F2 was placed in the TurboVap II® at 23ºC and concentrated to 100-200 µL, after which it was transferred to the GC-MS vials, ready for *n*-alkanes and PAHs analysis. F2 was also placed in the TurboVap II® at the same temperature for sample reduction.

2.2.6. Derivatization

The F2 samples were derivatized before the analysis of fecal and plant sterol: which need to be converted to a more volatile suitable for the GC-MS. Each sample was evaporated to dryness using nitrogen, then 100 µL of N,O-Bis(trimethylsilyl)trifluoroacetamide + 1% trimethylchlorosilane (BSTFA+1% TMCS) and 100 µL of DCM were added. Samples were heated at 70 °C for 1 hour in a Thermo block, after which the samples were left to cool and attain room temperature, then transferred into the GC-MS vials ready for the GC-MS analysis; as explained in (Battistel *et al.*, 2015). Each sample was injected into the GC-MS machine for analysis, 24 hours after derivatization for stability.

2.3. Quantification

2.3.1. *n*-Alkanes analysis

The *n*-alkanes analysis was carried out with the GC-MS. 2 µL of sample were injected in the equipment, the temperature at 300°C with a splitless mode.

***n*-alkanes quantification** Each chromatogram was integrated using the response factor retention times as the standard for comparison. *m/z* 71 was used to quantify the *n*-alkanes in the range C_{12}-C_{35}.

2.3.2. Polycyclic Aromatic Hydrocarbons

PAHs analysis was carried out using GC-MS. Samples were injected in splitless mode (split valve open after 1.5 min), and the inlet and interface temperature was 300 °C Helium was used as carrier gas at 1 mL min-1 flow. The oven temperature was programmed from 70 ^{0}C (isothermal for 1.5 min) to 150 ^{0}C at 10 $^\circ$C min^{-1}, then to 300 ^{0}C at 3 $^\circ$C min^{-1} (15 min). The temperature was

kept at 305 °C for 30 minutes of post run. Helium was used as carrier gas at the constant flow of 1.0 mL min^{-1}. The inlet and interface temperature was held at 300 ˚C. The ion source and quadrupole mass analyzer was kept at 230 ˚C and 150 ˚C, respectively. The mass analyzer was operated in Single Ion Monitoring (SIM) mode in order to identify specific ion/charge (*m/z*) ratios.

Polycyclic aromatic hydrocarbon quantification

19 polycyclic aromatic hydrocarbons were analyzed, using 3 different internal standards. The light molecular weight PAHs (3 rings) were quantified with the ^{13}C-Acenaphthylene, the middle molecular weight PAHs were quantified with ^{13}C-Phenantrene, and the heavy molecular weights were quantified with ^{13}C-Benzo(*a*)Pyrene.

Table 2.1. PAHs analyzed with respect to the internal standard used for each category.

Light molecular weights PAHs		
Compound name	**Molecular weight** g/mol	**Response factor**
Naphthalene	128	**Acenaphthylene ^{13}C**
Acenaphthylene	152	
Acenaphthene	154	
Fluorene	166	
Mid molecular weight PAHs		
Compound name	**Molecular weight g/mol**	**Response factor**
Phenanthrene	178	**Phenanthrene ^{13}C**
Anthracene	178	
Fluoranthene	202	
Pyrene	202	
Benzo(a)Anthracene	228	
Chrysene	228	
Retene	234	
Heavy molecular weight PAHs (5-6 rings PAHs)		

Compound name	Molecular weight	Response factor
Benzo(b)Fluoranthene	252	**Benzo(a)Pyrene ^{13}C**
Benzo(k)Fluoranthene	252	
Benzo(e)Pyrene	252	
Benzo(a)Pyrene	252	
Perylene	252	
Benzo(ghi)Perylene	276	
Indeno(1,2,3-c,d)Pyrene	276	
Dibenzo(A, H)Anthracene	278	

Response factor was injected three times for every batch of samples (14 samples) injected into the GC-MS, the average of the three-response factor was calculated and used for the quantification of the samples injected the same day. The area of each a compound was divided by area of the internal standard, then multiplied by the internal standard divided by the total average of response factor.

Absolute values where corrected for the mean blank and divided by the sample dry weight to get the final concentrations.

2.3.4. Monosaccharide anhydrides

Monosaccharide anhydride was separated into levoglucosan, mannosan and galactosan with ion-chromatography and mass spectrometry. A NaOH solution was used as carrier, with a 0.250 mL min^{-1} flow. The gradient was as follows: 20 mM (0-15 min), 100 mM (15-40 min), 20 mM (40-60 min). The source was operated in negative mode and the temperature was 350 °C. The needle and cone voltages were -3.5 kV and -50 V. The target ion for quantification was *m/z* 161 and qualifiers were *m/z* 110 and 113 (Kirchgeorg et al. 2014).

Method summary

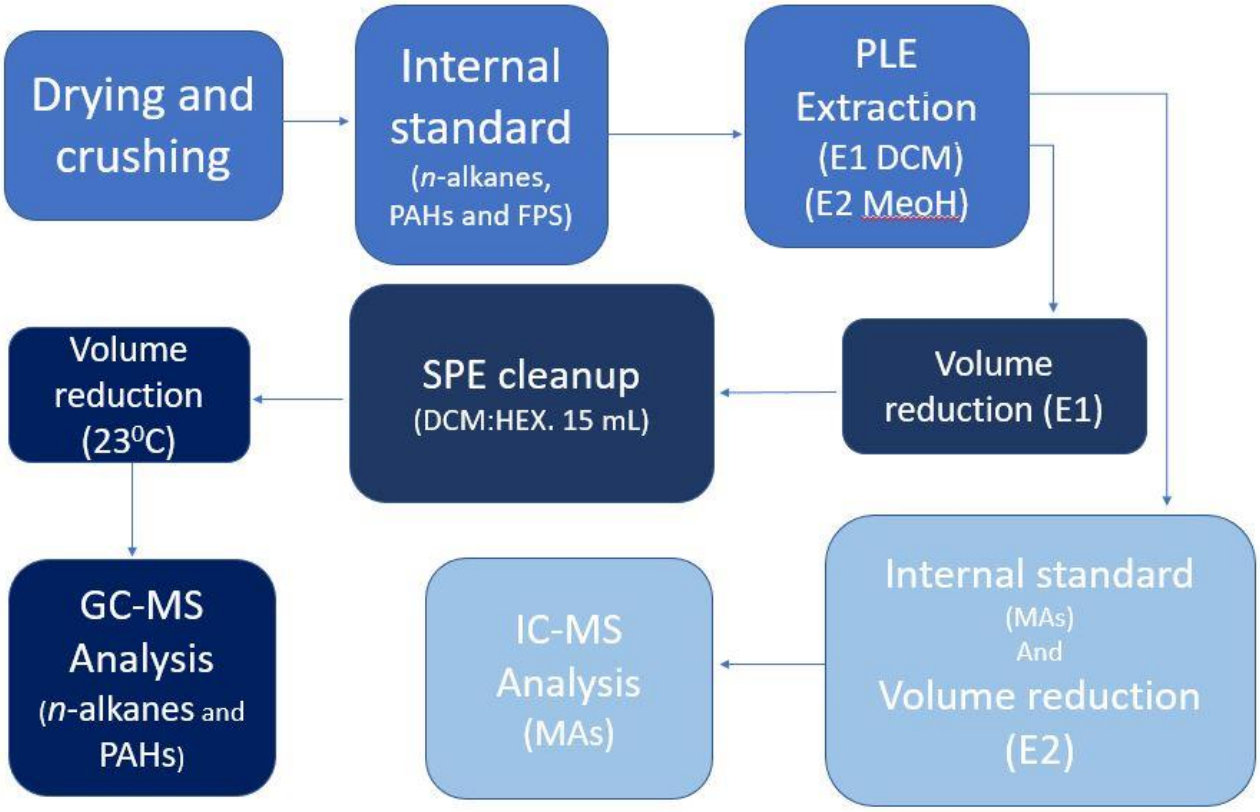

Fig.2.8. Diagram showing methods procedures.

3. RESULTS

The age-depth model in fig 3.1 shows a linear relationship between depth and age, which implies a quite constant sedimentation rate without discontinuity. *n*-Alkanes, polycyclic aromatic hydrocarbons and monosaccharide anhydrides were analyzed to determine fire regime and vegetation distribution. The analytical results were normalized with Z-score, the age-depth model was used to discuss the vegetation distribution and fire episodes in the MIS-5.

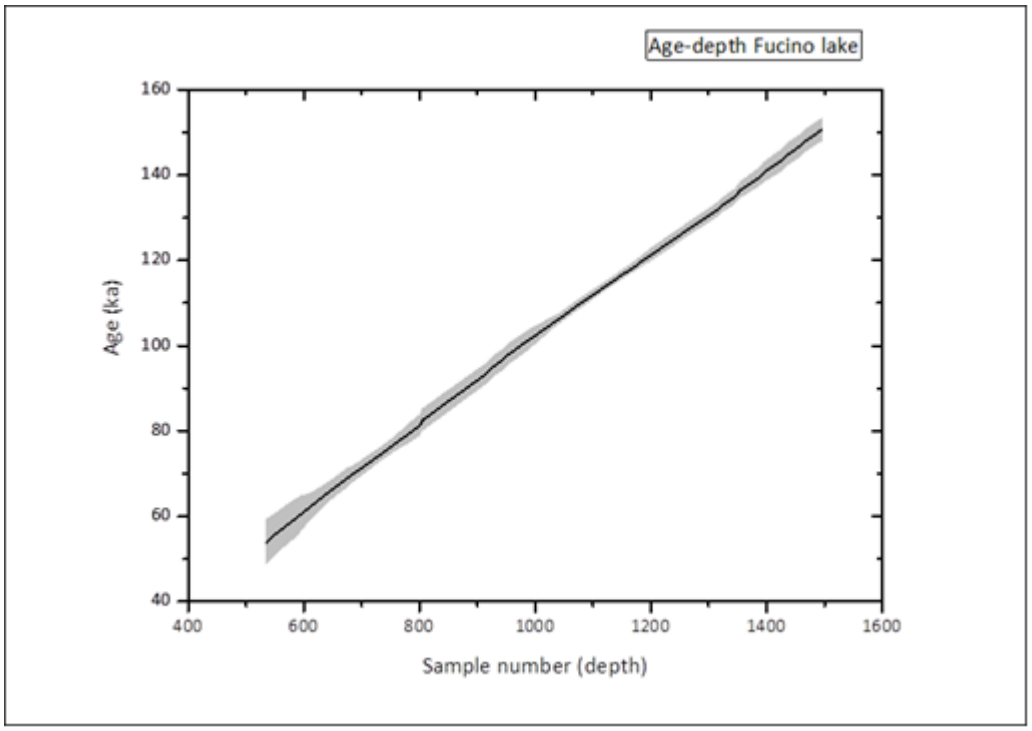

Fig.3.1. Age-depth model for the Lake Fucino core (grey area represents the age uncertainty).

n-Alkanes

The *n*-alkanes detected in the analysis were between C_{12} to C_{35}. Different indexes were calculated in other to be able to reconstruct vegetation distribution.

The Long-Chain *n*-alkanes (LCH)

Long-chain n-alkanes (LCH > C_{23}) are employed for inferring past vegetation types: by dividing odd long chain n-alkanes by the total amount of n-alkanes. The length of the alkane carbon chain strongly depends on the vegetation type, and longer chain alkanes are produced mainly by leaf wax of terrestrial plants. Although it is not species-specific, this method is useful for understanding vegetation sources of alkanes in sediments. LCH is produced by plants during warm environmental period. The value of LCH also helps in understanding shift in environmental condition and shift in vegetation (El Nemr *et al.*, 2016).

- $LCH = \frac{nC_{27} + nC_{29} + nC_{31} + nC_{33}}{\sum Ch}$

C_{27} and C_{29} are produced by shrubs and woody plants leaf wax (Bakhtiari *et al.*, 2010, El Nemr *et al.*, 2016). As reported in Fig.3.1, LCH record in characterized by an initial period where the major contribution of alkanes was provided by long hydrocarbon chains (from 1380 to 91).

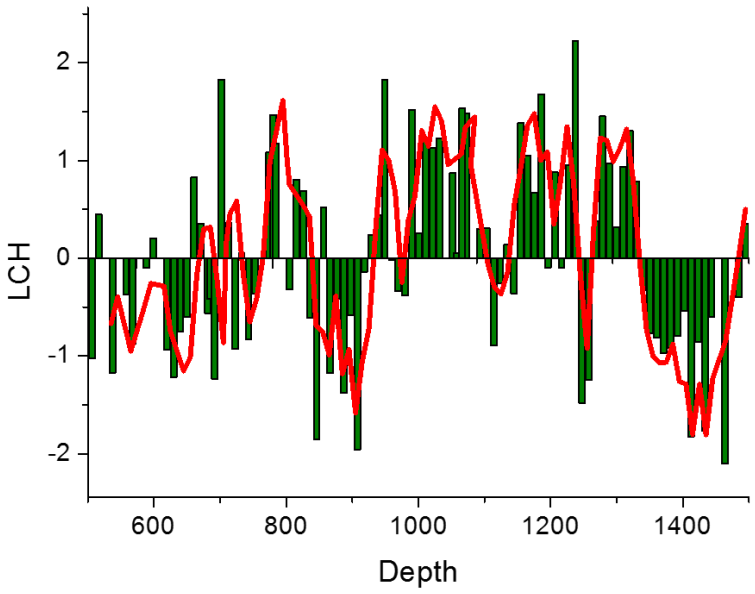

Fig 3.2. Long-chain n-alkanes (LCH > C_{23}) in Lake Fucino core.

Terrigenous/aquatic ratio (TAR)

Terrigenous aquatic ratio (TAR), is used for the quantification of terrestrial plants vs aquatic plants. (Hoş-Çebi, 2017). Long chains n-alkanes with an odd number of carbon atoms (C_{27}, C_{29}, and C_{31}) are produced from higher plants (terrestrial plants) waxes as mentioned previously, while aquatic plants produce odd short-chain *n*-alkanes. The ratio between the short and long chain *n*-alkanes is the Terrigenous/aquatic ratio (TAR), this ratio is used to access sediment vegetation source, comparing the terrestrial input with that of the aquatic input High value of TAR is an indication of terrestrial source and reduced/negative value of TAR indicates aquatic source (El Nemr *et al.*, 2016).

- $TAR = \frac{C_{27} + C_{29} + C_{31}}{C_{15} + C_{17} + C_{19}}$

The calculated TAR index shows an oscillation between terrestrial input and aquatic input, aquatic source dominates between the depth of 500 to 700, while terrestrial dominates between 700 to 800, from 820 to 920 is dominated by aquatic plants, then terrestrial plants dominates from 920 to 1200, which is followed by the dominance of aquatic plants to 1400.

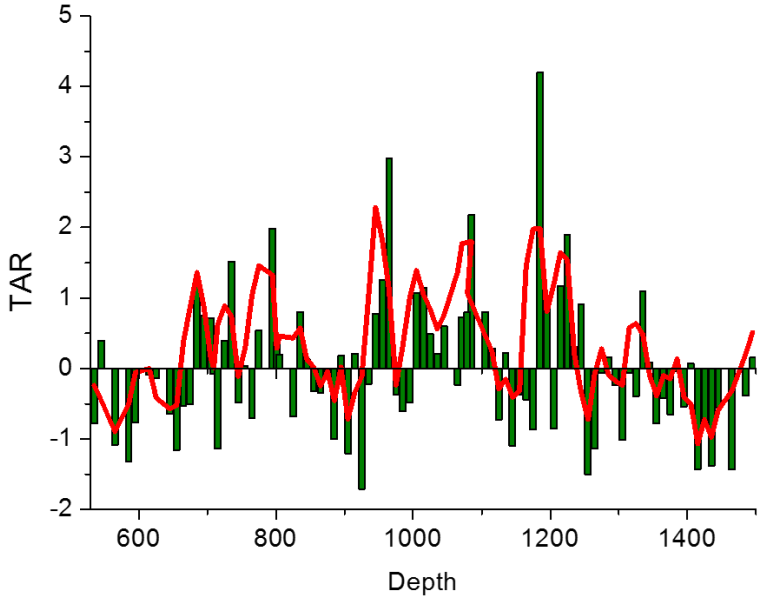

Fig. 3.3. Terrigenous/aquatic ratio with a moving average for *n*-alkanes in Lake Fucino.

Polycyclic aromatic hydrocarbon (PAHs)

The PAHs were divided the number of rings: 3 and 4 rings were summed together and 5-ring PAHs were also grouped to get a more significant result. The graphs of all the PAHs are shown below.

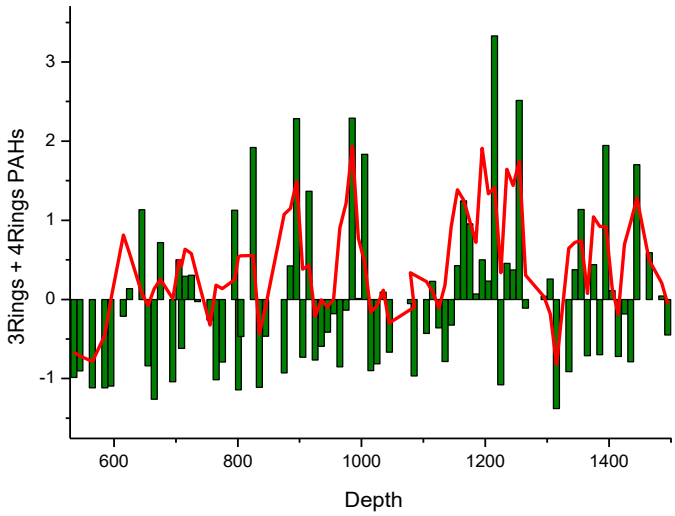

Fig.3.4. 3+4-ring PAHs concentrations in Lake Fucino core.

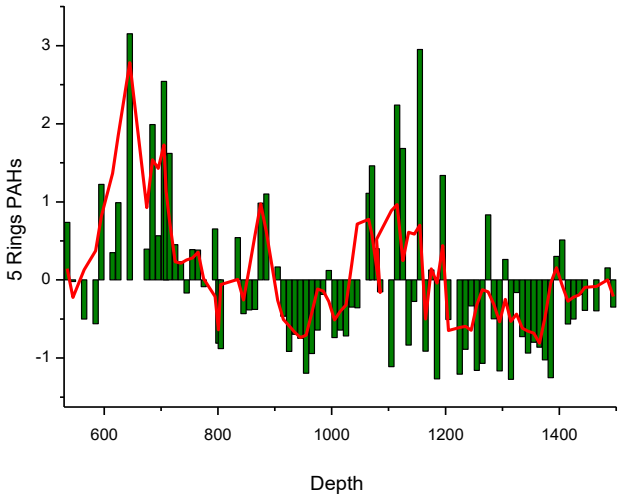

Fig.3.5. Plot Sum of 5-rings PAHs concentrations in Lake Fucino core.

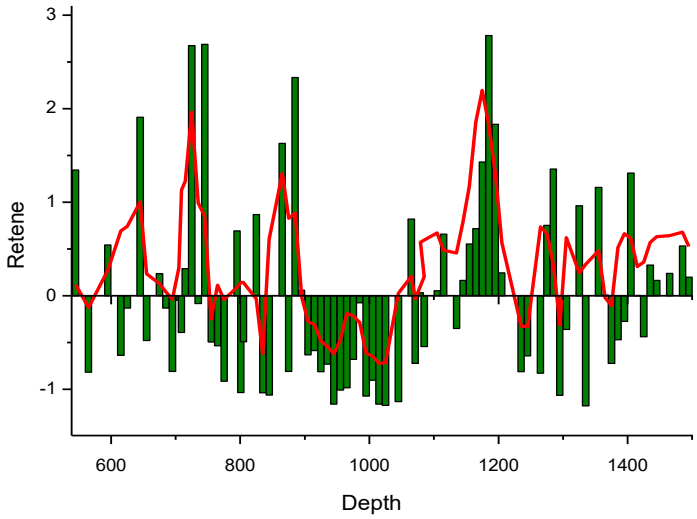

Fig.3.6. Retene concentrations in Lake Fucino core.

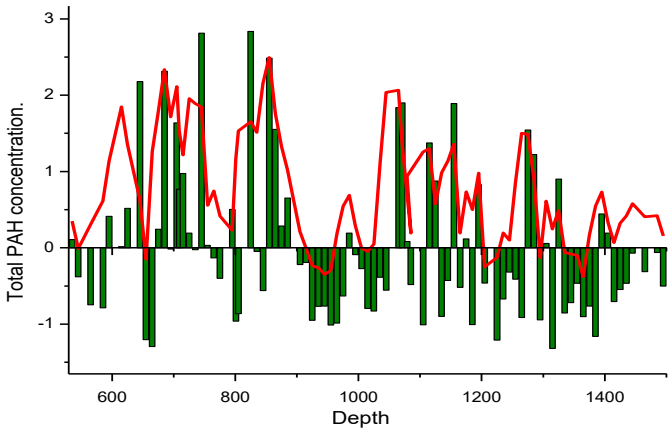

Fig.3.7. Total PAH concentration in Lake Fucino core.

Monosaccharide anhydrides

Levoglucosan, mannosan, and galactosan were summed together to form a single graph.

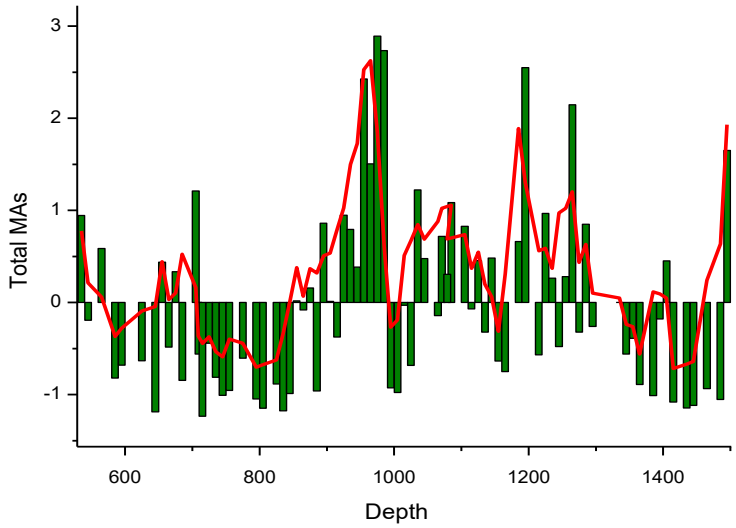

Fig.3.8. Total MAs concentration in Lake Fucino core.

The graph result of monosaccharide anhydrides shows oscillation signals, but there is a sharp increase in the concentration between the depth of 900-1000.

3. DISCUSSION

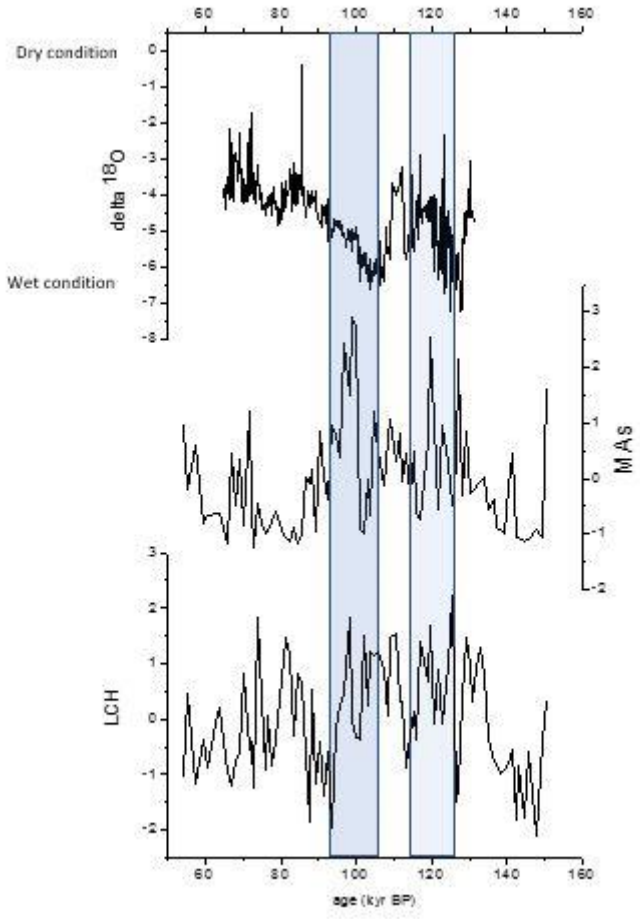

Fig 4.1. Comparison of discussed proxies LCH and MAs from current study. $\delta^{18}O$ (Mannella et al in, preparation).

4.1 Vegetation Distribution

4.1.2. Long-chain n-alkanes (LCH > C_{23})

The indices calculated for *n*-alkanes were used for classifying vegetation distribution. The long chain *n*-alkanes LCH shows a higher concentration between 130 -95 kyr BP, LCH is formed from the wax of woody plants, shrubs, and grass, as stated in the result section. High values of LCH indicate high level of terrestrial plants (El Nemr *et al.*, 2016). This indicates that there was a lot of terrestrial plant biomass (trees, grass, and shrubs) between 130 kyr BP

and 95 kyr BP. The LCH record can also be used for to determine the climatic condition within the period (Bakhtiari *et al.*, 2010). Woody plants and grasses can only thrive in a specific climatic condition. For example, biomes that have a very low temperature such as the tundra and taiga biome lack woody plants and grass, because the temperature is too low to support plant growth, the growing season is short that the grass that manages to grow up there are dwarfs. Biomes with warmer climates such as rainforest or temperate forest support grass and woody plants: the warmer climates allows higher terrestrial plants to thrive (Seki *et al.*, 2009; Wu, Chen and Huang, 2011; Tipple *et al.*, 2015; Margalef *et al.*, 2017; Sannigrahi, 2017). Judging by this explanation, plants produce longer-chain *n*-alkanes during warm climatic and environmental condition. The high concentration of the LCH is an indication of high terrestrial plant activity and also indicates that the climatic condition between 130-95 kyr BP was warm.

4.1.2. Terrigenous/aquatic ratio (TAR)

It has been stressed in this report that predominance value of odd *n*-alkanes number (C_{27}, C_{29}, C_{31}) is an indicator of higher terrestrial plants, while predominance value of odd *n*-alkanes number such as (C_{15}, C_{17} and C_{19}) are formed from aquatic plants wax, which indicates aquatic biomass. The terrestrial/aquatic ratios (TAR), is used to determine the input of *n*-alkanes from these two sources, comparing the long chain *n*-alkanes and the short chain *n*-alkanes (El Nemr *et al.*, 2016). The graph of the TAR shows an alternating value between LCH and SCH. This record shows that the biomass activity during the MIS-5 was higher both the terrestrial and aquatic source. although they both dominates at a different time and period.

4.2 Fire reconstruction

Monosaccharide anhydrides were summed together, fig 4.1. shows two episode of fire activities, between 130, to 120, kyr BP, and between 100 to 90 kyr BP. There was no fire event before 130 kyr BP. levoglucosan concentrations increasing from 130 kyr BP, which is an indication of fire activities. The higher intensity of the fire is between 103 to 92 kyr BP. The MAs record is also an indication of dry environmental condition. (Fraser, 2000, Marlon *et al.*, 2013, Kirchgeorg *et al.*, 2014).

4.3 Precipitation

Oxygen isotope ($\delta^{18}O$)

The oxygen isotope results displayed in this report were adopted from an ongoing paper by Mannuella et *al* (in preparation), being that the authors carried out the oxygen isotopic analysis on the same samples from Lake Fucino. $\delta^{18}O$ was used to compare the vegetation distribution and fire events in order to investigate the correlation between the proxies. The indication of a warmer period suggested by *n*-alkanes and monosaccharide anhydrides should be supported by direct indicators of climate conditions, in order to test the suitability of the tracers used for the Fucino record. Oxygen isotope is a reliable proxy for reconstructing climate condition such as precipitation, water balance and atmospheric circulation, this is because of the close link between the precipitation composition of oxygen isotope ($\delta^{18}O_P$) and the parameters of climates, decreased value of $\delta^{18}O$ is an indication of high precipitation, warm and wet environment. (Jonsson *et al.*, 2010). The interpretation of $\delta^{18}O$ in the lake sediments in comparison with that of the *n*-alkanes previously discussed, provides a reliable reconstruction of lake level and other climate parameters, like temperature and precipitation.

Low values of $\delta^{18}O$ indicate increased moisture conditions, high lake productivity and increased precipitation, it also means higher catchment erosion (Nehme *et al.*, 2015). The $\delta^{18}O$ shows a low value in the mid MIS-5 from 130, kya BP and begins to increase by100 kya BP, with quick increase and decrease between 115 to 117 kya BP, in agreement with the *n*-alkanes record.

4.4. Polycyclic Aromatic Hydrocarbons (PAHs)

Retene was the most abundant PAH found in the sediment. Low molecular weight PAHs were grouped together (3-ring and 4-ring PAHs). Higher molecular weight PAHs were also

grouped together (5 rings PAHs), Retene is often used to indicate combustion of conifer plants, as it is the main PAH emission form the combustion of softwood, and it might not be detected in samples that have been exposed to photoreaction (Simoneit, 2002). It can also be detected in samples from region where conifers are not common because retene is not always generated from combustion, it can be sometimes generated through biological processes, under the condition of anoxic in the lake (Yunker *et al.*, 2002, Musa Bandowe *et al.*, 2014). However, due to low concentrations and high variation of the PAHs could not be used to infer or reconstruct fire activity.

4.5. Comparison of the proxies

Comparison between $\delta^{18}O$, monosaccharide anhydrides and *n*-alkanes indices shows positive correlation. The three proxies show activities between 130 kyr BP to 90 kyr BP, $\delta^{18}O$ indicates high precipitation from 130 kyr BP to 100 kyr BP. High precipitation is often the result of warm climatic condition, which in turn is favorable for vegetation growth, especially plants with wax that produces long chain *n*-alkanes (trees, shrubs and grass). This explains why there is high vegetation between 130 to 90 kyr BP. The graph shows fire activity between 102 to 92 kyr BP. There are specific climatic and environmental conditions that support natural fire activities without anthropogenic influence. The first condition that supports wildfire is when the concentration of atmospheric O_2 is >13%, the second condition is when there is dry climate, and the third condition is the availability of biomass to act as fuel. From the n-alkanes record discussed above, we find out that there was abundance terrestrial vegetation to serve as fuel to be burnt, and the $\delta^{18}O$ record show a gradual decrease in precipitation from 103kya BP, therefore indicating movement to a dry environments (Kehrwald *et al.*, 2010; Marlon *et al.*, 2013). The graph shows that the fire activity became intensified soon after the decreased in precipitation, where vegetation can easily lead to wildfire as a result of natural triggers e.g. lightning.

Two intervals can be defined from the graph, although the first is not so evident as the second. The gradual decrease in precipitation by 125 kyr BP resulted in immediate fire activity. There was rise in precipitation again and it begins to drop for the second time around 102,000yr BP, this was followed by an immediate intensified fire activity. the graph also shows a decrease in vegetation after each fire periods.

The $\delta^{18}O$ record is therefore in agreement with the fire and vegetation record of this study, showing a cause-effect relationship between the climatic variables.

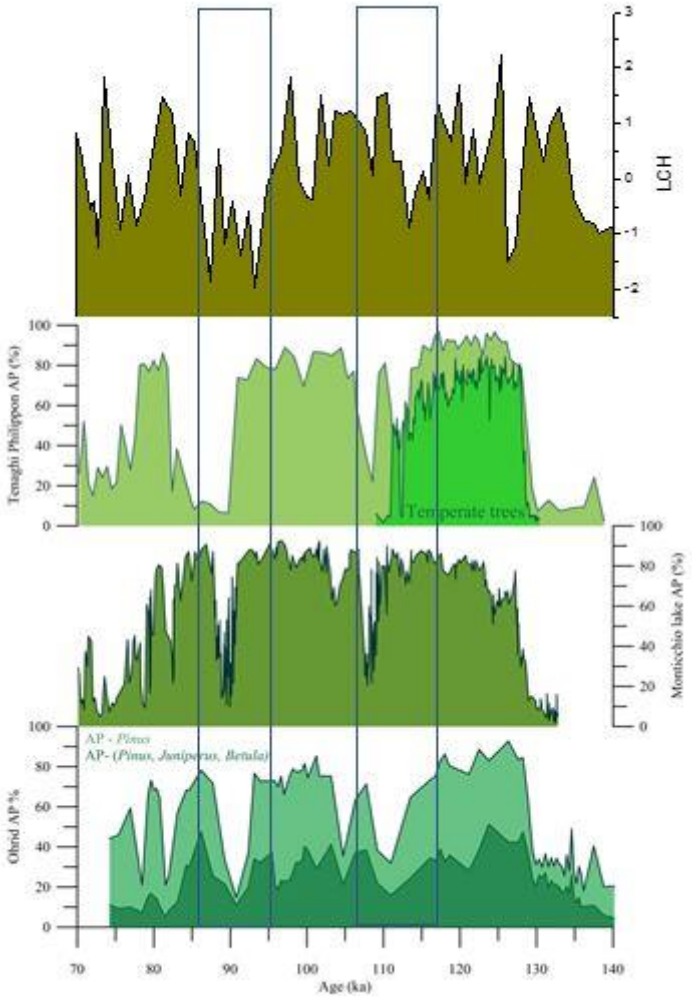

Fig 4.7. From bottom: DEEP Tenaghi Philippon,%of temperate trees from Milner et al. (2012) plotted on chronology;Monticchio site pollen record (AP-Pinus and AP-(Pinus, Betula and Juniperus), LCH current study (Sadori et al., 2016; Zanchetta *et al.*, 2015)

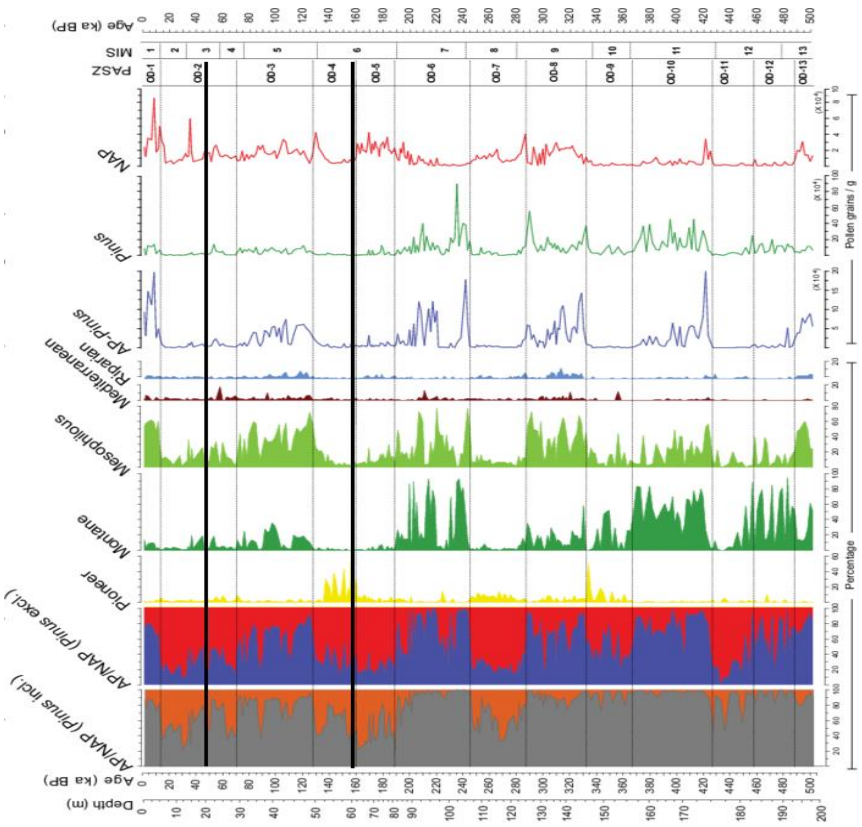

Fig.4.8. Deep core. pollen from lake Ohrid, Albania. (Francke *et al.*, 2016; Sadori *et al.*, 2016).

Images above display the results obtained from other research papers compared with LCH of this study. The images where adopted from a study from lake ohrid in Albania, the pollen records is in agreement with the terrestrial vegetation records from this study, with little lag, this might be as a result of sedimentation dynamics, age model or the distance between the lake locations. The report by Sadori *et al.*, 2016 stated that the MIS5 (129, -70 kyr BP) was dominated by higher terrestrial plants, such as decidious and semi decidious forest (Sadori *et al.*, 2016). Another research from the Mediterranean region suggest that the MIS-5 displayed a very high primary productivity in the epilimnion of Lake Ohrid, with very high temperatures during spring and summer, which have been described to be the warmest among interglacial periods (Francke *et al.*, 2016).

4. CONCLUSION

GC-MS and IC-MS was very useful in performance the separation of organic biomarkers. PAHs were not significantly stable; hence it was not useful for the discussion of this research. The benefit of multiple proxy analysis in paleoenvironmental studies cannot be overemphasized, as some of the proxies might not give a useful result for environmental reconstruction. However, the monosaccharide anhydrides (levoglucosan) show a very interesting signal and were also a very significant proxy for this research, since this is the first time the MAs and PAHs have been used for fire event reconstruction in lake sediment in the MIS-5. The MAs record was also positively correlated with that of the long chain *n*-alkanes, therefore supporting the idea of more frequent fires sustained by abundance fuel.

The current results also agree with results derived from different proxies from other researches in the Mediterranean region. From the result discussed in this study, the MIS-5 has a high vegetation activity, warm and wet environment, and high precipitation. There were also fire episodes, which reduced the vegetation for a while. It also indicates that humans are not the only cause of wildfire, as human were not present during the MIS-5, but there are presence of fire episodes.

Reference

Ab, B. (2010) ‘TurboVap II User’s Manual’.

Abdel-Shafy, H. I. and Mansour, M. S. M. (2015) ‘A review on polycyclic aromatic hydrocarbons: Source, environmental impact, effect on human health and remediation’, *Egyptian Journal of Petroleum*. Egyptian Petroleum Research Institute, 25(1), pp. 107–123. doi: 10.1016/j.ejpe.2015.03.011.

Amann, B., Mauchle, F. and Grosjean, M. (2014) ‘Quantitative high-resolution warm season rainfall recorded in varved sediments of Lake Oeschinen, northern Swiss Alps: Calibration and validation AD 1901-2008’, *Journal of Paleolimnology*, 51(3), pp. 375–391. doi: 10.1007/s10933-013-9761-3.

Badejo, a. O., Choi, B.-H., Cho, H.-G., Yi, H.-I. and Shin, K.-H. (2014) ‘A paleoenvironmental reconstruction of the last 15 000 cal yr BP via Yellow Sea sediments using biomarkers and isotopic composition of organic matter’, *Climate of the Past Discussions*, 10(2), pp. 1527–1565. doi: 10.5194/cpd-10-1527-2014.

Baek, S. O., Field, R. A., Goldstone, M. E., Kirk, P. W., Lester, J. N. and Perry, R. (1991) ‘A review of atmospheric polycyclic aromatic hydrocarbons: Sources, fate and behavior’, *Water, Air, and Soil Pollution*, 60(3–4), pp. 279–300. doi: 10.1007/BF00282628.

Bakhtiari, A. R., Zakaria, M. P., Yaziz, M. I., Lajis, M. N. H., Bi, X., Shafiee, M. R. M. and Sakari, M. (2010) ‘Distribution of PAHS and n-alkanes in Klang River Surface Sediments, Malaysia’, *Pertanika Journal of Science and Technology*, 18(1), pp. 167–179.

Ball, A. (1996) ‘Using Faecal Sterols From Humans and Animals To Distinguish Faecal Pollution in Receiving Waters’, 30(12), pp. 2893–2900.

Battistel, D., Piazza, R., Argiriadis, E., Marchiori, E., Radaelli, M. and Barbante, C. (2015) ‘GC-MS method for determining faecal sterols as biomarkers of human and pastoral animal presence in freshwater sediments’, *Analytical and bioanalytical chemistry*, 407(28), pp. 8505–8514. doi: 10.1007/s00216-015-8998-2.

Birks, H. (2011) ‘Introduction to Quaternary Palaeoecology’, pp. 1–10.

Bowman Jennifer K. Balch, Paulo Artaxo, William J. Bond, Jean M. Carlson, Mark A. Cochrane, Carla M. D'Antonio, Ruth S. DeFries, John C. Doyle, Sandy P. Harrison, Fay H. Johnston, Jon E. Keeley, Meg A. Krawchuk, Christian A. Kull, J. Brad Marston, Max A., D. M. J. . (2009) 'Fire in the Earth System', *Science*, 324, pp. 481–484. doi: 10.1126/science.1163886.

Bruckner, M. (2017) *Paleoclimatology: How Can We Infer Past Climates?* Available at: http://serc.carleton.edu/microbelife/topics/proxies/paleoclimate.html.

Bull, I. D., Matthew J. Lockheart, Mohamed M. Elhmmali, David J. Roberts and Richard P. Evershed (2002) ', Evershed RP (2002) The Origin of Faeces by Means of Biomarker Detection. Environ Int - Google Scholar', *Environment International*, 27(8), pp. 647–654. Available at: https://scholar.google.de/scholar?hl=en&q=%2C+Evershed+RP+%282002%29+The+Origin+of+Faeces+by+Means+of+Biomarker+Detection.+Environ+Int&btnG=&as_sdt=1%2C5&as_sdtp=.

Bull, I. D., Simpson, I. a., van Bergen, P. F. and Evershed, R. P. (1999) 'Muck'n'molecules: organic geochemical methods for detecting ancient manuring', *Antiquity*, 3(June 1998), pp. 86–96. doi: 10.1017/S0003598X0008786X.

Cañellas-Boltà, N., Rull, V., Sáez, A., Margalef, O., Giralt, S., Pueyo, J. J., Birks, H. H., Birks, H. J. B. and Pla-Rabes, S. (2012) 'Macrofossils in Raraku Lake (Easter Island) integrated with sedimentary and geochemical records: Towards a palaeoecological synthesis for the last 34,000 years', *Quaternary Science Reviews*. Elsevier Ltd, 34, pp. 113–126. doi: 10.1016/j.quascirev.2011.12.013.

Castañeda, I. S. and Schouten, S. (2011) 'A review of molecular organic proxies for examining modern and ancient lacustrine environments', *Quaternary Science Reviews*. Elsevier Ltd, 30(21–22), pp. 2851–2891. doi: 10.1016/j.quascirev.2011.07.009.

Cavinato, G. P., Carusi, C., Dall'asta, M., Miccadei, E. and Piacentini, T. (2002) 'Sedimentary and tectonic evolution of Plio-Pleistocene alluvial and lacustrine deposits of Fucino Basin (central Italy)', *Sedimentary Geology*, 148(1–2), pp. 29–59. doi: 10.1016/S0037-0738(01)00209-3.

D'Anjou, R. M., Bradley, R. S., Balascio, N. L. and Finkelstein, D. B. (2012) 'Climate impacts on human settlement and agricultural activities in northern Norway revealed through sediment biogeochemistry.', *Proceedings of the National Academy of Sciences of the United States of America*, 109(50), pp. 20332–20337. doi: 10.1073/pnas.1212730109.

Denis, E. H., Toney, J. L., Tarozo, R., Scott Anderson, R., Roach, L. D. and Huang, Y. (2012) 'Polycyclic aromatic hydrocarbons (PAHs) in lake sediments record historic fire events: Validation using HPLC-fluorescence detection', *Organic Geochemistry*. Elsevier Ltd, 45, pp. 7–17. doi: 10.1016/j.orggeochem.2012.01.005.

Francke, A., Wagner, B., Just, J., Leicher, N., Gromig, R., Baumgarten, H., Vogel, H., Lacey, J. H., Sadori, L., Wonik, T., Leng, M. J., Zanchetta, G., Sulpizio, R. and Giaccio, B. (2016) 'Sedimentological processes and environmental variability at Lake Ohrid (Macedonia, Albania) between 637 ka and the present', *Biogeosciences*, 13(4), pp. 1179–1196. doi: 10.5194/bg-13-1179-2016.

Fraser, M. P. (2000) 'Using Levoglucosan as a Molecular Marker for the Long-Range Transport of Biomass Combustion Aerosols', 34(21), pp. 4560–4564.

Fraser, M. P. and Lakshmanan, K. (2000) 'Using levoglucosan as a molecular marker for the long-range transport of biomass combustion aerosols', *Environmental Science and Technology*, 34(21), pp. 4560–4564. doi: 10.1021/es991229l.

Fritz, S. C. (2008) 'Deciphering climatic history from lake sediments', *Journal of Paleolimnology*, 39(1), pp. 5–16. doi: 10.1007/s10933-007-9134-x.

Giaccio, B., Niespolo, E. M., Pereira, A., Nomade, S., Renne, P. R., Albert, P. G., Arienzo, I., Regattieri, E., Wagner, B., Zanchetta, G., Gaeta, M., Galli, P., Mannella, G., Peronace, E., Sottili, G., Florindo, F., Leicher, N., Marra, F. and Tomlinson, E. L. (2017) 'First integrated tephrochronological record for the last ~190 kyr from the Fucino Quaternary lacustrine succession, central Italy', *Quaternary Science Reviews*. Elsevier Ltd, 158, pp. 211–234. doi: 10.1016/j.quascirev.2017.01.004.

Giaccio, B., Regattieri, E., Zanchetta, G., Wagner, B., Galli, P., Mannella, G., Niespolo, E., Peronace, E., Renne, P. R., Nomade, S., Cavinato, G. P., Messina, P., Sposato, A., Boschi, C., Florindo, F., Marra, F. and Sadori, L. (2015) '11A key continental archive for the last

2Ma of climatic history of the central Mediterranean region: A pilot drilling in the Fucino Basin, central Italy', *Scientific Drilling*, 20, pp. 13–19. doi: 10.5194/sd-20-13-2015.

Holtvoeth, J., Vogel, H., Wagner, B. and Wolff, G. A. (2010) 'Lipid biomarkers in Holocene and glacial sediments from ancient Lake Ohrid (Macedonia, Albania)', *Biogeosciences*, 7(11), pp. 3473–3489. doi: 10.5194/bg-7-3473-2010.

Hoş-Çebi, F. (2017) 'Organic geochemical characteristics and paleoclimate conditions of the Miocene coals at the Çan-Durali (Çanakkale)', *Journal of African Earth Sciences*, 129. doi: 10.1016/j.jafrearsci.2016.12.003.

Hsu, C. L., Cheng, C. Y., Lee, C. T. and Ding, W. H. (2007) 'Derivatization procedures and determination of levoglucosan and related monosaccharide anhydrides in atmospheric aerosols by gas chromatography-mass spectrometry', *Talanta*, 72(1), pp. 199–205. doi: 10.1016/j.talanta.2006.10.018.

IPCC Climate Change (2007) *The Physical Science Basis. Contribution of Working Group I to the Fourth Assessment Report of the Intergovernmental Panel on Climate Change. Solomon, S., Quin, D., Manning, M., Chen, Z., Marquis, M., Tignor, K. B. M. and Miller, H. L. (eds), Cambridge Un*.

Jenkins, B. M., Jones, a D., Turn, S. Q. and Williams, R. B. (1996) 'Emission factors for polycyclic aromatic hydrocarbons from biomass burning', *Environmental Science & Technology*, 30(8), pp. 2462–2469. doi: 10.1021/es950699m.

Jimenez, J., Farias, O., Quiroz, R. and Yañez, J. (2017) 'Emission factors of particulate matter, Polycyclic Aromatic Hydrocarbons and Levoglucosan from wood combustion in South Central Chile', *Journal of the Air & Waste Management Association*. Taylor & Francis, 67(7), p. 10962247.2017.1295114. doi: 10.1080/10962247.2017.1295114.

Jimenez, J. L., Canagaratna, M. R. and Worsnop, D. R. (2009) 'Evolution of Organic Aerosols in the Atmosphere', *Science*, 326(5959), pp. 1525–1529. doi: 10.1126/science.1180353.

Jonsson, C. E., Andersson, S., Rosqvist, G. C. and Leng, M. J. (2010) 'Reconstructing past atmospheric circulation changes using oxygen isotopes in lake sediments from Sweden', *Climate Of The Past*, 6(1), pp. 49–62. doi: 10.5194/cp-6-49-2010.

Jordan, T. B., Seen, A. J. and Jacobsen, G. E. (2006) 'Levoglucosan as an atmospheric tracer for woodsmoke', *Atmospheric Environment*, 40(27), pp. 5316–5321. doi: 10.1016/j.atmosenv.2006.03.023.

Kehrwald, N., Zangrando, R., Gambaro, A. and Barbante, C. (2010) 'Fire and climate: Biomass burning recorded in ice and lake cores', *EPJ Web of Conferences*. EDP Sciences, 9, pp. 105–114. doi: 10.1051/epjconf/201009008.

Khedidji, S., Balducci, C., Ladji, R., Cecinato, A., Perilli, M. and Yassaa, N. (2017) 'Chemical composition of particulate organic matter at industrial, university and forest areas located in Bouira province, Algeria', *Atmospheric Pollution Research*. Elsevier Ltd, 8(3), pp. 474–482. doi: 10.1016/j.apr.2016.12.005.

Kirchgeorg, T., Schüpbach, S., Kehrwald, N., McWethy, D. B. and Barbante, C. (2014) 'Method for the determination of specific molecular markers of biomass burning in lake sediments', *Organic Geochemistry*. Elsevier Ltd, 71, pp. 1–6. doi: 10.1016/j.orggeochem.2014.02.014.

Lacey, J. H., Leng, M. J., Francke, A., Sloane, H. H., Milodowski, A., Vogel, H., Baumgarten, H., Zanchetta, G. and Wagner, B. (2016) 'Northern Mediterranean climate since the Middle Pleistocene: A 637 ka stable isotope record from Lake Ohrid (Albania/Macedonia)', *Biogeosciences*, 13(6), pp. 1801–1820. doi: 10.5194/bg-13-1801-2016.

Last, W. M. and Smol, J. P. (2002) *Tracking Environmental Change Using Lake Sediments. Volume 2: Physical and Geochemical Methods, Book*. doi: 10.1007/0-306-47670-3_5.

Lazier, J. R. N. (1995) *Natural Climate Variability on Decade-to-Century Time Scales*, *Natural Climate Variability on Decade-to-Century Time Scales*. doi: 10.17226/5142.

Li, B., Nychka, D. W. and Ammann, C. M. (2010) 'The Value of Multiproxy Reconstruction of Past Climate', *Journal of the American Statistical Association*, 105(491), pp. 883–895. doi: 10.1198/jasa.2010.ap09379.

Margalef, O., Sardans, J., Fernández-Martínez, M., Molowny-Horas, R., Janssens, I. A., Ciais, P., Goll, D., Richter, A., Obersteiner, M., Asensio, D. and Peñuelas, J. (2017) 'Global patterns of phosphatase activity in natural soils', *Scientific Reports*, 7(1), p. 1337. doi:

10.1038/s41598-017-01418-8.

Marlon, J. R., Bartlein, P. J., Daniau, A. L., Harrison, S. P., Maezumi, S. Y., Power, M. J., Tinner, W. and Vanniére, B. (2013) 'Global biomass burning: A synthesis and review of Holocene paleofire records and their controls', *Quaternary Science Reviews*. Elsevier Ltd, 65, pp. 5–25. doi: 10.1016/j.quascirev.2012.11.029.

Masson-Delmotte, V., Schulz, M., Abe-Ouchi, A., Beer, J., Ganopolski, A., Rouco, G., Fidel, J., Jansen, E., Lambeck, K., Luterbacher, J., Naish, T., Osborn, T., Otto-Bliesner, B. L., Quinn, T., Ramesh, R., Rojas, M., Shao, X. and Timmermann, A. (2015) 'IPCC Chapter 5 : Informations from paleoclimate archives, powerpoint presentation', *Climate Change 2013: The Physical Science Basis. Contribution of Working Group I to the Fifth Assessment Report of the Intergovernmental Panel on Climate Change*, p. 89.

Milner, A. M., Roucoux, K. H., Collier, R. E. L., M??ller, U. C., Pross, J. and Tzedakis, P. C. (2016) 'Vegetation responses to abrupt climatic changes during the Last Interglacial Complex (Marine Isotope Stage 5) at Tenaghi Philippon, NE Greece', *Quaternary Science Reviews*. Elsevier Ltd, 154, pp. 169–181. doi: 10.1016/j.quascirev.2016.10.016.

Monica Bruckner (2017) *Paleoclimatology: How Can We Infer Past Climates?*

Musa Bandowe, B. A., Srinivasan, P., Seelge, M., Sirocko, F. and Wilcke, W. (2014) 'A 2600-year record of past polycyclic aromatic hydrocarbons (PAHs) deposition at Holzmaar (Eifel, Germany)', *Palaeogeography, Palaeoclimatology, Palaeoecology*. Elsevier B.V., 401, pp. 111–121. doi: 10.1016/j.palaeo.2014.02.021.

Nehme, C., Verheyden, S., Noble, S. R., Farrant, A. R., Sahy, D., Hellstrom, J., Delannoy, J. J. and Claeys, P. (2015) 'Reconstruction of MIS 5 climate in the central Levant using a stalagmite from Kanaan Cave, Lebanon', *Climate of the Past*, 11(12), pp. 1785–1799. doi: 10.5194/cp-11-1785-2015.

Nelson, G. H. J. and Fussmann, G. F. (2002) 'Lake ecosystems', *Encyclopedia of Life Science*, pp. 1–3.

El Nemr, A., Moneer, A. A., Ragab, S. and El Sikaily, A. (2016) 'Distribution and sources of n-alkanes and polycyclic aromatic hydrocarbons in shellfish of the Egyptian Red Sea coast', *Egyptian Journal of Aquatic Research*. National Institute of Oceanography and Fisheries,

42(2), pp. 121–131. doi: 10.1016/j.ejar.2016.05.003.

Obuseng, V. C. and Nareetsile, F. (2013) 'Bile Acids As Specific Faecal Pollution Indicators in Water and Sediments', *European Scientific Journal,* 9(12), pp. 273–286.

Ouyang, X., Guo, F. and Bu, H. (2015) 'Lipid biomarkers and pertinent indices from aquatic environment record paleoclimate and paleoenvironment changes', *Quaternary Science Reviews*. Elsevier Ltd, 123, pp. 180–192. doi: 10.1016/j.quascirev.2015.06.029.

Pampanin, D. M. and Sydnes, M. O. (2013) 'Polycyclic Aromatic Hydrocarbons a Constituent of Petroleum : Presence and Influence in the Aquatic Environment', *Intech*, pp. 83–118. doi: 10.5772/48176.

Preparation, M. et al in (2017) 'personal contact'.

Ravindra, K., Sokhi, R. and Van Grieken, R. (2008) 'Atmospheric polycyclic aromatic hydrocarbons: Source attribution, emission factors and regulation', *Atmospheric Environment*, 42(13), pp. 2895–2921. doi: 10.1016/j.atmosenv.2007.12.010.

Regattieri, E., Giaccio, B., Nomade, S., Francke, A., Vogel, H., Drysdale, R. N., Perchiazzi, N., Wagner, B., Gemelli, M., Mazzini, I., Boschi, C., Galli, P. and Peronace, E. (2017) '11 A Last Interglacial record of environmental changes from the Sulmona Basin (central Italy)', *Palaeogeography, Palaeoclimatology, Palaeoecology*. Elsevier B.V., 472, pp. 51–66. doi: 10.1016/j.palaeo.2017.02.013.

Richter, H., Benish, T. G., Mazyar, O. A., Green, W. H. and Howard, J. B. (2000) 'Formation of Polycyclic Aromatic Hydrocarbons and their Radicals in a Nearly Sooting Premixed Benzene Flame', *Proceedings of the Combustion Institute*, 28(2), pp. 2609–2618. doi: 10.1016/S0082-0784(00)80679-7.

Sadori, L., Koutsodendris, A., Panagiotopoulos, K., Masi, A., Bertini, A., Combourieu-Nebout, N., Francke, A., Kouli, K., Joannin, S., Mercuri, A. M., Peyron, O., Torri, P., Wagner, B., Zanchetta, G., Sinopoli, G. and Donders, T. H. (2016) 'Pollen-based paleoenvironmental and paleoclimatic change at Lake Ohrid (south-eastern Europe) during the past 500 ka', *Biogeosciences*, 13(5), pp. 1423–1437. doi: 10.5194/bg-13-1423-2016.

Sánez, J., Froehner, S., Hansel, F., Parron, L., Knapik, H., Fernandes, C. and Rizzi, J. (2017)

‘Bile acids combined with fecal sterols: a multiple biomarker approach for deciphering fecal pollution using river sediments’, *Journal of Soils and Sediments*. Journal of Soils and Sediments, 17(3), pp. 861–872. doi: 10.1007/s11368-016-1592-1.

Sannigrahi, S. (2017) ‘Modeling terrestrial ecosystem productivity of an estuarine ecosystem in the Sundarban Biosphere Region, India using seven ecosystem models’, *Ecological Modelling*. Elsevier B.V., 356, pp. 73–90. doi: 10.1016/j.ecolmodel.2017.03.003.

Schellekens, J. and Buurman, P. (2011) ‘N-Alkane distributions as palaeoclimatic proxies in ombrotrophic peat: The role of decomposition and dominant vegetation’, *Geoderma*. Elsevier B.V., 164(3–4), pp. 112–121. doi: 10.1016/j.geoderma.2011.05.012.

Schüpbach, S., Kirchgeorg, T., Colombaroli, D., Beffa, G., Radaelli, M., Kehrwald, N. M. and Barbante, C. (2015) ‘Combining charcoal sediment and molecular markers to infer a Holocene fire history in the Maya Lowlands of Pet??n, Guatemala’, *Quaternary Science Reviews*. Elsevier Ltd, 115, pp. 123–131. doi: 10.1016/j.quascirev.2015.03.004.

Scientific, T. F. (2017) ‘Thermo Fisher Scientific’. Available at: https://www.thermofisher.com.

Seki, O., Meyers, P. A., Kawamura, K., Zheng, Y. and Zhou, W. (2009) ‘Hydrogen isotopic ratios of plant wax n-alkanes in a peat bog deposited in northeast China during the last 16 kyr’, *Organic Geochemistry*. Elsevier Ltd, 40(6), pp. 671–677. doi: 10.1016/j.orggeochem.2009.03.007.

Simoneit, B. R. T. (2002) *Biomass burning - A review of organic tracers for smoke from incomplete combustion*, *Applied Geochemistry*. doi: 10.1016/S0883-2927(01)00061-0.

Simoneit, B. R. T., Schauer, J. J., Nolte, C. G., Oros, D. R., Elias, V. O., Fraser, M. P., Rogge, W. F. and Cass, G. R. (1999) ‘Levoglucosan, a tracer for cellulose in biomass burning and atmospheric particles’, *Atmospheric Environment*, 33(2), pp. 173–182. doi: 10.1016/S1352-2310(98)00145-9.

Thermo, T., Dionex, S. and Accelerated, A. S. E. (no date) ‘Thermo Scientific Dionex ASE 150 Accelerated Solvent Extractor System’, pp. 60–61.

Tipple, B. J., Berke, M. A., Hambach, B., Roden, J. S. and Ehleringer, J. R. (2015)

‘Predicting leaf wax n-alkane $^{2}H/^{1}H$ ratios: Controlled water source and humidity experiments with hydroponically grown trees confirm predictions of Craig-Gordon model’, *Plant, Cell and Environment*, 38(6), pp. 1035–1047. doi: 10.1111/pce.12457.

Tomassetti, B., Giorgi, F., Verdecchia, M. and Visconti, G. (2003) ‘Regional model simulation of the hydrometeorological effects of the Fucino Lake on the surrounding region’, *Annales Geophysicae*, 21, pp. 2219–2232. doi: 10.5194/angeo-21-2219-2003.

WHO (2000) ‘Air quality guidelines for Europe’, *Environmental Science and Pollution Research*, 3(1), pp. 23–23. doi: 10.1007/BF02986808.

Wu, C., Chen, J. M. and Huang, N. (2011) ‘Predicting gross primary production from the enhanced vegetation index and photosynthetically active radiation: Evaluation and calibration’, *Remote Sensing of Environment*. Elsevier Inc., 115(12), pp. 3424–3435. doi: 10.1016/j.rse.2011.08.006.

Yang, C. R., Lin, T. C. and Chang, F. H. (2007) ‘Particle size distribution and PAH concentrations of incense smoke in a combustion chamber’, *Environmental Pollution*, 145(2), pp. 606–615. doi: 10.1016/j.envpol.2005.10.036.

Yunker, M. B., Macdonald, R. W., Vingarzan, R., Mitchell, R. H., Goyette, D. and Sylvestre, S. (2002) ‘PAHs in the Fraser River basin: A critical appraisal of PAH ratios as indicators of PAH source and composition’, *Organic Geochemistry*, 33(4), pp. 489–515. doi: 10.1016/S0146-6380(02)00002-5.

Zanchetta, G., Regattieri, E., Giaccio, B., Wagner, B., Sulpizio, R., Francke, A., Vogel, L. H., Sadori, L., Masi, A., Sinopoli, G., Lacey, J. H., Leng, M. L. and Leicher, N. (2015) ‘11Aligning MIS5 proxy records from Lake Ohrid (FYROM) with independently dated Mediterranean archives: Implications for core chronology’, *Biogeosciences Discussions*, 12(20), pp. 16979–17007. doi: 10.5194/bgd-12-16979-2015.

Zhang, Y., Zheng, M., Meyers, P. A. and Huang, X. (2017) ‘Impact of early diagenesis on distributions of Sphagnum n-alkanes in peatlands of the monsoon region of China’, *Organic Geochemistry*. Elsevier Ltd, 105, pp. 13–19. doi: 10.1016/j.orggeochem.2016.12.007.

Appendix

n-Alkanes indices calculated with a 10 years interval.

Depth	Age (Cal yr BP)	Forest vs Grassland	LCH	TAR
535	53	0.77	0.16	3.00
585	59	0.90	0.24	1.39
625	63	0.84	0.31	4.95
675	68	1.08	0.22	3.83
725	73	1.31	0.51	6.55
775	78	1.46	0.25	7.01
825	83	1.42	0.25	3.31
875	88	1.58	0.35	4.92
925	93	2.99	0.05	0.20
965	98	1.18	0.51	14.40
1025	103	1.31	0.44	6.86
1071	108	1.34	0.30	7.56
1125	113	1.36	0.18	3.17
1185	118	0.87	0.37	18.06
1235	124	0.99	0.40	6.28
1275	128	1.15	0.33	5.16
1325	133	0.83	0.45	4.18
1375	138	1.14	0.17	3.40
1425	143	0.90	0.18	2.97
1485	149	0.82	0.24	4.21

PAHs concentrations with a 10 years interval.

Depth	Age (Cal yr BP)	3 Rings PAHs	4 Rings PAHs	5 Rings PAHs
535	53	10.68		167.68
585	59	5.23	2.00	59.46
625	63	24.20	16.38	188.73
675	68	31.62	24.43	139.07
725	73	26.50	18.60	143.89
775	78	10.23	5.66	99.18
825	83	46.96	41.09	430.33

875	88	10.11	2.12	188.20
925	93	11.72	4.88	29.93
965	98	10.93	3.38	27.65
1025	103	11.21	4.06	46.42
1071	108	171.56	1.76	228.18
1125	113	16.97	10.39	246.62
1185	118	17.87	20.90	0.54
1235	124	12.63	36.49	32.10
1275	128	157.41	24.11	175.73
1325	133	174.49	9.92	92.74
1375	138	14.25	34.42	20.96
1425	143	25.39	6.65	64.60
1485	149	23.82	14.33	119.07

Contraction index calculated for FPS

Depth	AGE (Cal yr BP)	Cop + e-cop	Sit + 5α-Sit
555	56	0.85	2.44
655	67	0.79	0.21
765	78	3.06	3.44
855	87	2.89	1.69
945	97	8.23	6.48
1065	109	3.57	4.80
1175	119	2.24	2.84
1275	128	5.18	5.69
1285	129	13.29	22.74
1385	139	1.06	0.49
1485	150	5.73	9.99

Tables of the indices calculated in this research

Mean	0.288913681	0.288913681
Dev st	0.121219252	0.121219252
ouelier>	NO	
LHC		

# n	Age	LHC	- outlier	LHC	- outlier	Err 20%	Err 20%	LHC	-oulier	LHC	-oulier
				Z-score	Z-score	Z-score	Z-score	movav3	movav5	movav5	movav5
625	63.74	0.31	0.31	0.21	0.21	0.04	0.04	-0.65	-0.65	-0.66	-0.66
645	65.88	0.18	0.18	-0.94	-0.94	-0.19	-0.19	-0.97	-0.97	-0.54	-0.54
655	66.91	0.14	0.14	-1.21	-1.21	-0.24	-0.24	-0.86	-0.86	-0.28	-0.28

665	67.93	0.20	0.20	-0.75	-0.75	-0.15	-0.15	-0.18	-0.18	-0.15	-0.15
675	68.94	0.22	0.22	-0.61	-0.61	-0.12	-0.12	0.19	0.19	-0.08	-0.08
685	69.92	0.39	0.39	0.83	0.83	0.17	0.17	0.20	0.20	-0.21	-0.21
695	70.80	0.33	0.33	0.35	0.35	0.07	0.07	-0.21	-0.21	-0.01	-0.01
705	71.80	0.22	0.22	-0.56	-0.56	-0.11	-0.11	-0.74	-0.74	-0.01	-0.01
709	72.19	0.24	0.24	-0.42	-0.42	-0.08	-0.08	0.06	0.06	-0.08	-0.08
715	72.75	0.14	0.14	-1.24	-1.24	-0.25	-0.25	0.32	0.32	0.02	0.02
725	73.74	0.51	0.51	1.83	1.83	0.37	0.37	0.42	0.42	0.10	0.10
735	74.73	0.33	0.33	0.36	0.36	0.07	0.07	-0.17	-0.17	-0.34	-0.34
745	75.71	0.18	0.18	-0.93	-0.93	-0.19	-0.19	-0.57	-0.57	-0.20	-0.20
755	76.71	0.30	0.30	0.06	0.06	0.01	0.01	-0.38	-0.38	0.28	0.28
765	77.71	0.19	0.19	-0.83	-0.83	-0.17	-0.17	-0.03	-0.03	0.51	0.51
775	78.72	0.25	0.25	-0.36	-0.36	-0.07	-0.07	0.73	0.73	0.61	0.61
795	80.72	0.42	0.42	1.08	1.08	0.22	0.22	1.24	1.24	0.84	0.84
801	81.32	0.47	0.47	1.47	1.47	0.29	0.29	0.77	0.77	0.76	0.76
805	82.50	0.43	0.43	1.18	1.18	0.24	0.24	0.55	0.55	0.35	0.35
825	83.50	0.25	0.25	-0.32	-0.32	-0.06	-0.06	0.39	0.39	-0.26	-0.26
835	84.50	0.39	0.39	0.80	0.80	0.16	0.16	0.29	0.29	-0.09	-0.09
845	85.49	0.37	0.37	0.69	0.69	0.14	0.14	-0.59	-0.59	-0.49	-0.49
855	86.47	0.21	0.21	-0.62	-0.62	-0.12	-0.12	-0.65	-0.65	-0.71	-0.71
865	87.45	0.06	0.06	-1.85	-1.85	-0.37	-0.37	-0.84	-0.84	-0.86	-0.86
875	88.42	0.35	0.35	0.52	0.52	0.10	0.10	-0.36	-0.36	-0.61	-0.61
885	89.39	0.15	0.15	-1.18	-1.18	-0.24	-0.24	-0.99	-0.99	-1.10	-1.10
895	90.41	0.24	0.24	-0.42	-0.42	-0.08	-0.08	-0.79	-0.79	-0.90	-0.90
905	91.38	0.12	0.12	-1.38	-1.38	-0.28	-0.28	-1.31	-1.31	-0.77	-0.77
915	92.35	0.22	0.22	-0.59	-0.59	-0.12	-0.12	-0.90	-0.90	-0.40	-0.40
925	93.32	0.05	0.05	-1.96	-1.96	-0.39	-0.39	-0.62	-0.62	0.08	0.08
935	94.79	0.27	0.27	-0.14	-0.14	-0.03	-0.03	0.18	0.18	0.47	0.47
945	95.78	0.32	0.32	0.24	0.24	0.05	0.05	0.84	0.84	0.43	0.43
955	96.78	0.34	0.34	0.44	0.44	0.09	0.09	0.75	0.75	0.31	0.31
965	98.05	0.51	0.51	1.83	1.83	0.37	0.37	0.49	0.49	0.52	0.52
975	99.03	0.29	0.29	-0.02	-0.02	0.00	0.00	-0.25	-0.25	0.21	0.21
985	100.00	0.25	0.25	-0.34	-0.34	-0.07	-0.07	0.27	0.27	0.45	0.45
995	100.95	0.24	0.24	-0.38	-0.38	-0.08	-0.08	0.46	0.46	0.75	0.75
1005	101.91	0.47	0.47	1.52	1.52	0.30	0.30	1.00	1.00	1.07	1.07
1015	102.85	0.32	0.32	0.25	0.25	0.05	0.05	0.87	0.87	0.94	0.94
1025	103.80	0.44	0.44	1.22	1.22	0.24	0.24	1.19	1.19	0.90	0.90
1035	104.75	0.43	0.43	1.13	1.13	0.23	0.23	1.07	1.07	0.95	0.95
1045	105.68	0.44	0.44	1.23	1.23	0.25	0.25	0.72	0.72	1.03	1.03
1065	107.54	0.39	0.39	0.87	0.87	0.17	0.17	0.80	0.80	0.85	0.85
1071	108.64	0.30	0.30	0.05	0.05	0.01	0.01	1.02	1.02	0.73	0.73
1085	109.20	0.47	0.47	1.48	1.48	0.30	0.30	1.11	1.11	0.54	0.54
1079	110.50	0.47	0.47	1.53	1.53	0.31	0.31	0.71	0.71	0.20	0.20
1105	111.43	0.33	0.33	0.30	0.30	0.06	0.06	-0.10	-0.10	-0.08	-0.08

1115	112.37	0.33	0.33	0.30	0.30	0.06	0.06	-0.28	-0.28	-0.22	-0.22
1125	113.30	0.18	0.18	-0.90	-0.90	-0.18	-0.18	-0.34	-0.34	0.00	0.00
1135	114.24	0.26	0.26	-0.26	-0.26	-0.05	-0.05	-0.16	-0.16	0.39	0.39
1145	115.17	0.31	0.31	0.14	0.14	0.03	0.03	0.39	0.39	0.58	0.58
1155	116.10	0.24	0.24	-0.36	-0.36	-0.07	-0.07	0.69	0.69	0.88	0.88
1245	125.42	0.56	0.56	2.22	2.22	0.44	0.44	-0.17	-0.17	0.26	0.26
1255	126.35	0.11	0.11	-1.48	-1.48	-0.30	-0.30	-0.78	-0.78	0.02	0.02
1265	127.28	0.14	0.14	-1.25	-1.25	-0.25	-0.25	0.19	0.19	0.37	0.37
1275	128.21	0.33	0.33	0.38	0.38	0.08	0.08	0.93	0.93	0.81	0.81
1285	129.04	0.46	0.46	1.45	1.45	0.29	0.29	0.91	0.91	1.00	1.00
1295	129.97	0.41	0.41	0.97	0.97	0.19	0.19	0.74	0.74	0.86	0.86
1305	130.89	0.33	0.33	0.32	0.32	0.06	0.06	0.85	0.85	0.60	0.60
1315	131.82	0.40	0.40	0.93	0.93	0.19	0.19	1.01	1.01	0.39	0.39
1325	133.02	0.45	0.45	1.30	1.30	0.26	0.26	0.59	0.59	0.04	0.04
1335	133.95	0.38	0.38	0.79	0.79	0.16	0.16	-0.10	-0.10	-0.42	-0.42
1345	134.88	0.25	0.25	-0.32	-0.32	-0.06	-0.06	-0.63	-0.63	-0.76	-0.76
1355	136.49	0.20	0.20	-0.77	-0.77	-0.15	-0.15	-0.85	-0.85	-0.85	-0.85
1365	137.41	0.19	0.19	-0.82	-0.82	-0.16	-0.16	-0.90	-0.90	-0.81	-0.81
1375	138.32	0.17	0.17	-0.97	-0.97	-0.19	-0.19	-0.90	-0.90	-1.01	-1.01
1385	139.23	0.18	0.18	-0.92	-0.92	-0.18	-0.18	-0.75	-0.75	-0.99	-0.99
1395	140.56	0.19	0.19	-0.80	-0.80	-0.16	-0.16	-1.05	-1.05	-1.16	-1.16
1445	145.57	0.22	0.22	-0.60	-0.60	-0.12	-0.12	-1.03	-1.03	-0.69	-0.69
1465	147.80	0.03	0.03	-2.10	-2.10	-0.42	-0.42	-0.72	-0.72	-0.72	-0.72
1485	149.62	0.24	0.24	-0.40	-0.40	-0.08	-0.08	-0.02	-0.02	-0.02	-0.02
1495	150.52	0.33	0.33	0.35	0.35	0.07	0.07	0.35	0.35	0.35	0.35

Z-score for TAR.

Mean	5.365203857	5.365203857
Dev st	3.024298482	3.024298482
ouelier>	NO	
TAR		

						TAR	outlier				
# n	Age	TAR	- outlier	TAR	- outlier	Err 20%	Err 20%	TAR	-oulier	TAR	-oulier
				Z-score	Z-score	Z-score	Z-score	movav3	movav5	movav5	movav5
615	62.66	5.09	5.09	-0.09	-0.09	-0.02	-0.02	-0.29	-0.29	-0.51	-0.51
625	63.74	4.95	4.95	-0.14	-0.14	-0.03	-0.03	-0.64	-0.64	-0.59	-0.59
645	65.88	3.45	3.45	-0.63	-0.63	-0.13	-0.13	-0.77	-0.77	-0.33	-0.33
655	66.91	1.87	1.87	-1.16	-1.16	-0.23	-0.23	-0.73	-0.73	-0.05	-0.05
665	67.93	3.75	3.75	-0.53	-0.53	-0.11	-0.11	0.05	0.05	0.32	0.32
675	68.94	3.83	3.83	-0.51	-0.51	-0.10	-0.10	0.47	0.47	0.41	0.41
685	69.92	8.92	8.92	1.18	1.18	0.24	0.24	0.88	0.88	0.29	0.29
695	70.80	7.64	7.64	0.75	0.75	0.15	0.15	0.46	0.46	0.13	0.13

705	71.80	7.53	7.53	0.71	0.71	0.14	0.14	-0.17	-0.17	0.28	0.28
709	72.19	5.13	5.13	-0.08	-0.08	-0.02	-0.02	-0.27	-0.27	0.04	0.04
715	72.75	1.92	1.92	-1.14	-1.14	-0.23	-0.23	0.26	0.26	0.06	0.06
725	73.74	6.55	6.55	0.39	0.39	0.08	0.08	0.47	0.47	0.15	0.15
735	74.73	9.94	9.94	1.51	1.51	0.30	0.30	0.36	0.36	0.18	0.18
745	75.71	3.91	3.91	-0.48	-0.48	-0.10	-0.10	-0.38	-0.38	0.28	0.28
755	76.71	5.49	5.49	0.04	0.04	0.01	0.01	-0.04	-0.04	0.45	0.45
765	77.71	3.23	3.23	-0.71	-0.71	-0.14	-0.14	0.61	0.61	0.48	0.48
775	78.72	7.01	7.01	0.54	0.54	0.11	0.11	0.97	0.97	0.48	0.48
795	80.72	11.37	11.37	1.98	1.98	0.40	0.40	0.85	0.85	0.54	0.54
801	81.32	6.48	6.48	0.37	0.37	0.07	0.07	-0.04	-0.04	0.17	0.17
805	82.50	5.97	5.97	0.20	0.20	0.04	0.04	0.11	0.11	0.03	0.03
825	83.50	3.31	3.31	-0.68	-0.68	-0.14	-0.14	0.09	0.09	-0.08	-0.08
835	84.50	7.80	7.80	0.81	0.81	0.16	0.16	0.21	0.21	0.03	0.03
845	85.49	5.76	5.76	0.13	0.13	0.03	0.03	-0.18	-0.18	-0.34	-0.34
855	86.47	4.41	4.41	-0.32	-0.32	-0.06	-0.06	-0.27	-0.27	-0.33	-0.33
865	87.45	4.33	4.33	-0.34	-0.34	-0.07	-0.07	-0.50	-0.50	-0.50	-0.50
875	88.42	4.92	4.92	-0.15	-0.15	-0.03	-0.03	-0.32	-0.32	-0.39	-0.39
885	89.39	2.32	2.32	-1.01	-1.01	-0.20	-0.20	-0.68	-0.68	-0.71	-0.71
895	90.41	5.92	5.92	0.18	0.18	0.04	0.04	-0.27	-0.27	-0.55	-0.55
905	91.38	1.71	1.71	-1.21	-1.21	-0.24	-0.24	-0.90	-0.90	-0.43	-0.43
915	92.35	6.00	6.00	0.21	0.21	0.04	0.04	-0.57	-0.57	0.06	0.06
925	93.32	0.20	0.20	-1.71	-1.71	-0.34	-0.34	-0.39	-0.39	0.62	0.62
935	94.79	4.69	4.69	-0.22	-0.22	-0.04	-0.04	0.60	0.60	0.88	0.88
945	95.78	7.70	7.70	0.77	0.77	0.15	0.15	1.67	1.67	0.81	0.81
955	96.78	9.16	9.16	1.26	1.26	0.25	0.25	1.29	1.29	0.56	0.56
965	98.05	14.40	14.40	2.99	2.99	0.60	0.60	0.67	0.67	0.52	0.52
975	99.03	4.24	4.24	-0.37	-0.37	-0.07	-0.07	-0.49	-0.49	0.15	0.15
985	100.00	3.53	3.53	-0.61	-0.61	-0.12	-0.12	0.00	0.00	0.33	0.33
995	100.95	3.93	3.93	-0.48	-0.48	-0.10	-0.10	0.58	0.58	0.49	0.49
1005	101.91	8.61	8.61	1.07	1.07	0.21	0.21	0.91	0.91	0.71	0.71
1015	102.85	8.85	8.85	1.15	1.15	0.23	0.23	0.62	0.62	0.45	0.45
1025	103.80	6.86	6.86	0.49	0.49	0.10	0.10	0.44	0.44	0.36	0.36
1035	104.75	6.00	6.00	0.21	0.21	0.04	0.04	0.19	0.19	0.70	0.70
1045	105.68	7.20	7.20	0.61	0.61	0.12	0.12	0.37	0.37	0.82	0.82
1065	107.54	4.66	4.66	-0.23	-0.23	-0.05	-0.05	0.89	0.89	0.85	0.85
1071	108.64	7.56	7.56	0.73	0.73	0.15	0.15	1.23	1.23	0.96	0.96
1085	109.20	11.95	11.95	2.18	2.18	0.44	0.44	1.26	1.26	0.67	0.67
1079	110.50	7.78	7.78	0.80	0.80	0.16	0.16	0.63	0.63	0.28	0.28
1105	111.43	7.77	7.77	0.80	0.80	0.16	0.16	0.12	0.12	-0.10	-0.10
1115	112.37	6.23	6.23	0.29	0.29	0.06	0.06	-0.07	-0.07	-0.34	-0.34
1125	113.30	3.17	3.17	-0.72	-0.72	-0.14	-0.14	-0.53	-0.53	-0.48	-0.48
1135	114.24	6.04	6.04	0.22	0.22	0.04	0.04	-0.42	-0.42	-0.51	-0.51
1145	115.17	2.04	2.04	-1.10	-1.10	-0.22	-0.22	-0.64	-0.64	0.28	0.28

1155	116.10	4.25	4.25	-0.37	-0.37	-0.07	-0.07	-0.56	-0.56	0.68	0.68
1165	117.04	4.04	4.04	-0.44	-0.44	-0.09	-0.09	0.96	0.96	0.59	0.59
1175	117.88	2.73	2.73	-0.87	-0.87	-0.17	-0.17	1.41	1.41	0.91	0.91
1185	118.81	18.06	18.06	4.20	4.20	0.84	0.84	1.41	1.41	1.46	1.46
1195	119.84	8.07	8.07	0.89	0.89	0.18	0.18	0.41	0.41	0.68	0.68
1265	127.28	1.92	1.92	-1.14	-1.14	-0.23	-0.23	-0.35	-0.35	-0.46	-0.46
1275	128.21	5.16	5.16	-0.07	-0.07	-0.01	-0.01	-0.05	-0.05	-0.24	-0.24
1285	129.04	5.85	5.85	0.16	0.16	0.03	0.03	-0.36	-0.36	-0.31	-0.31
1295	129.97	4.66	4.66	-0.23	-0.23	-0.05	-0.05	-0.44	-0.44	-0.12	-0.12
1305	130.89	2.31	2.31	-1.01	-1.01	-0.20	-0.20	-0.49	-0.49	-0.06	-0.06
1315	131.82	5.17	5.17	-0.06	-0.06	-0.01	-0.01	0.21	0.21	-0.01	-0.01
1325	133.02	4.18	4.18	-0.39	-0.39	-0.08	-0.08	0.26	0.26	-0.08	-0.08
1335	133.95	8.68	8.68	1.10	1.10	0.22	0.22	0.13	0.13	-0.14	-0.14
1345	134.88	5.61	5.61	0.08	0.08	0.02	0.02	-0.38	-0.38	-0.36	-0.36
1355	136.49	3.00	3.00	-0.78	-0.78	-0.16	-0.16	-0.62	-0.62	-0.49	-0.49
1365	137.41	4.08	4.08	-0.42	-0.42	-0.08	-0.08	-0.37	-0.37	-0.32	-0.32
1375	138.32	3.40	3.40	-0.65	-0.65	-0.13	-0.13	-0.41	-0.41	-0.52	-0.52
1385	139.23	5.24	5.24	-0.04	-0.04	-0.01	-0.01	-0.17	-0.17	-0.55	-0.55
1395	140.56	3.72	3.72	-0.54	-0.54	-0.11	-0.11	-0.63	-0.63	-0.81	-0.81
1495	150.52	5.83	5.83	0.15	0.15	0.03	0.03	0.15	0.15	0.15	0.15

Z-score Monosaccharide Anhydrides

Mean	18.18550943	16.57674697
Dev st	15.02626166	12.70781389
ouelier>	55	
MAs		

						MAs	-outlier				
# n	Age	MAs	-outlier	MAs	-outlier	Err 20%	MAs	TAR	-oulier	MAs	-oulier
				Z-score	Z-score	Z-score	Z-score	movav3	movav5	movav5	movav5
535	53.86	28.59	28.59	0.69	0.95	0.14	0.19	0.27	0.45	-0.13	-0.03
545	55.13	14.12	14.12	-0.27	-0.19	-0.05	-0.04	-0.23	-0.14	-0.34	-0.28
565	57.32	24.04	24.04	0.39	0.59	0.08	0.12	-0.36	-0.30	-0.43	-0.39
585	59.41	6.15	6.15	-0.80	-0.82	-0.16	-0.16	-0.74	-0.75	-0.81	-0.83
595	60.51	7.94	7.94	-0.68	-0.68	-0.14	-0.14	-0.66	-0.66	-0.54	-0.52
615	62.66										
625	63.74	8.53	8.53	-0.64	-0.63	-0.13	-0.13	-0.50	-0.46	-0.37	-0.31
645	65.88	1.50	1.50	-1.11	-1.19	-0.22	-0.24	-0.45	-0.41	-0.40	-0.35
655	66.91	22.15	22.15	0.26	0.44	0.05	0.09	-0.03	0.10	-0.22	-0.14

665	67.93	10.42	10.42	-0.52	-0.48	-0.10	-0.10	-0.39	-0.33	-0.06	0.05
675	68.94	20.84	20.84	0.18	0.34	0.04	0.07	-0.32	-0.26	-0.08	0.04
685	69.92	5.83	5.83	-0.82	-0.85	-0.16	-0.17	0.05	0.18	-0.41	-0.36
695	70.80										
705	71.80	31.97	31.97	0.92	1.21	0.18	0.24	-0.27	-0.19	-0.42	-0.37
709	72.19	9.46	9.46	-0.58	-0.56	-0.12	-0.11	-0.74	-0.75	-0.79	-0.81
715	72.75	0.88	0.88	-1.15	-1.23	-0.23	-0.25	-0.81	-0.83	-0.86	-0.89
725	73.74	10.98	10.98	-0.48	-0.44	-0.10	-0.09	-0.74	-0.75	-0.79	-0.80
735	74.73	6.27	6.27	-0.79	-0.81	-0.16	-0.16	-0.89	-0.92	-0.82	-0.84
745	75.71	3.78	3.78	-0.96	-1.01	-0.19	-0.20	-0.94	-0.98	-0.87	-0.90
755	76.71	4.43	4.43	-0.92	-0.96	-0.18	-0.19	-0.77	-0.78	-0.84	-0.87
765	77.71										
775	78.72	8.89	8.89	-0.62	-0.60	-0.12	-0.12	-0.81	-0.83	-0.89	-0.92
795	80.72	3.28	3.28	-0.99	-1.05	-0.20	-0.21	-1.04	-1.10	-1.01	-1.06
801	81.32										
805	82.50	1.98	1.98	-1.08	-1.15	-0.22	-0.23	-1.01	-1.07	-0.81	-0.84
825	83.50	5.34	5.34	-0.85	-0.88	-0.17	-0.18	-0.97	-1.02	-0.63	-0.62
835	84.50	1.65	1.65	-1.10	-1.17	-0.22	-0.23	-0.71	-0.72	-0.46	-0.41
845	85.49	4.00	4.00	-0.94	-0.99	-0.19	-0.20	-0.40	-0.35	-0.42	-0.37
855	86.47	16.80	16.80	-0.09	0.02	-0.02	0.00	-0.08	0.03	-0.11	0.00
865	87.45	15.55	15.55	-0.18	-0.08	-0.04	-0.02	-0.36	-0.30	-0.11	0.00
875	88.42	18.56	18.56	0.03	0.16	0.01	0.03	-0.09	0.02	-0.16	-0.06
885	89.39	4.36	4.36	-0.92	-0.96	-0.18	-0.19	-0.13	-0.03	-0.03	0.10
895	90.41	27.50	27.50	0.62	0.86	0.12	0.17	0.03	0.17	0.27	0.45
905	91.38	16.71	16.71	-0.10	0.01	-0.02	0.00	0.06	0.19	0.19	0.35
915	92.35	11.81	11.81	-0.42	-0.38	-0.08	-0.08	0.28	0.45	0.60	0.83
925	93.32	28.60	28.60	0.69	0.95	0.14	0.19	0.49	0.71	0.92	1.21
935	94.79	26.65	26.65	0.56	0.79	0.11	0.16	0.91	1.20	1.25	1.60
945	95.78	21.45	21.45	0.22	0.38	0.04	0.08	1.11	1.44	1.57	1.99
955	96.78	47.41	47.41	1.94	2.43	0.39	0.49	1.82	2.27	1.35	1.73
965	98.05	35.70	35.70	1.17	1.51	0.23	0.30	1.90	2.38	0.78	1.05
975	99.03	53.32	53.32	2.34	2.89	0.47	0.58	1.22	1.57	0.52	0.74
985	100.00	51.32	51.32	2.21	2.73	0.44	0.55	0.13	0.28	-0.09	0.02
995	100.95	4.82	4.82	-0.89	-0.93	-0.18	-0.19	-0.65	-0.65	-0.34	-0.28
1005	101.91	4.15	4.15	-0.93	-0.98	-0.19	-0.20	-0.58	-0.56	-0.11	0.00
1015	102.85	16.18	16.18	-0.13	-0.03	-0.03	-0.01	0.04	0.17	0.04	0.17
1025	103.80	7.90	7.90	-0.68	-0.68	-0.14	-0.14	0.18	0.34	0.16	0.32
1035	104.75	32.10	32.10	0.93	1.22	0.19	0.24	0.33	0.52	0.46	0.67
1045	105.68	22.64	22.64	0.30	0.48	0.06	0.10	0.19	0.35	0.31	0.49
1065	107.54	14.78	14.78	-0.23	-0.14	-0.05	-0.03	0.36	0.55	0.37	0.56
1071	108.64	25.71	25.71	0.50	0.72	0.10	0.14	0.49	0.70	0.38	0.57
1085	109.20	30.34	30.34	0.81	1.08	0.16	0.22	0.52	0.74	0.33	0.52
1079	110.50	20.47	20.47	0.15	0.31	0.03	0.06	0.19	0.35	0.10	0.24
1105	111.43	27.09	27.09	0.59	0.83	0.12	0.17	0.23	0.40	0.13	0.27

1115	112.37	15.69	15.69	-0.17	-0.07	-0.03	-0.01	-0.09	0.02	-0.12	-0.02
1125	113.30	22.36	22.36	0.28	0.46	0.06	0.09	0.07	0.21	-0.24	-0.15
1135	114.24	12.48	12.48	-0.38	-0.32	-0.08	-0.06	-0.24	-0.16	0.38	-0.31
1145	115.17	22.71	22.71	0.30	0.48	0.06	0.10	-0.36	-0.30	0.55	-0.06
1155	116.10	8.51	8.51	-0.64	-0.63	-0.13	-0.13	0.66	-0.69	0.90	0.46
1165	117.04	7.05	7.05	-0.74	-0.75	-0.15	-0.15	1.03	-0.04	1.52	0.82
1175	117.88	68.81		3.37		0.67		1.96		1.55	
1185	118.81	24.99	24.99	0.45	0.66	0.09	0.13	1.66	1.61	1.02	0.90
1195	119.84	48.99	48.99	2.05	2.55	0.41	0.51	1.31	0.99	0.95	0.80
1205	120.78	55.48		2.48		0.50		0.87		0.44	
1215	121.71	9.36	9.36	-0.59	-0.57	-0.12	-0.11	0.08	0.22	-0.03	0.09
1225	122.64	28.87	28.87	0.71	0.97	0.14	0.19	0.11	0.25	0.43	0.64
1235	124.49	19.93	19.93	0.12	0.26	0.02	0.05	-0.09	0.02	0.21	0.38
1245	125.42	10.50	10.50	-0.51	-0.48	-0.10	-0.10	0.44	0.65	0.31	0.50
1345	134.88	9.47	9.47	-0.58	-0.56	-0.12	-0.11	-0.63	-0.61	-0.05	-0.71
1355	136.49	11.63	11.63	-0.44	-0.39	-0.09	-0.08	0.44	-0.64	0.02	-0.62
1365	137.41	5.27	5.27	-0.86	-0.89	-0.17	-0.18	0.26	-0.95	0.16	-0.41
1375	138.32	57.36		2.61		0.52		0.46		0.13	
1385	139.23	3.74	3.74	-0.96	-1.01	-0.19	-0.20	-0.31	-0.25	-0.49	-0.45
1395	140.56	14.30	14.30	-0.26	-0.18	-0.05	-0.04	-0.33	-0.27	-0.52	-0.49
1405	141.46	22.33	22.33	0.28	0.45	0.06	0.09	-0.37	-0.31	-0.72	-0.72
1415	142.37	2.85	2.85	-1.02	-1.08	-0.20	-0.22	-1.05	-1.11	-1.01	-1.07
1495	150.52	37.55	37.55	1.29	1.65	0.26	0.33	1.29	1.65	1.29	1.65

Z-score of total Total sum of PAHs

Mean	177.785846	164.8151542
Dev st	150.8757425	124.669534
ouelier>	600	
PAHs		

						PAHs	-outlier				
# n	Age	PAHs	-outlier	PAHs	-outlier	Err 20%	Err 20%	PAHs	-oulier	PAHs	-oulier
				Z-score	Z-score	Z-score	Z-score	movav3	movav5	movav5	movav5
585	59.41	66.70	66.70	-0.74	-0.79	-0.15	-0.16	-0.19	-0.12	0.30	0.47
595	60.51	216.16	216.16	0.25	0.41	0.05	0.08	0.17	0.31	0.23	0.38
615	62.66	166.73	166.73	-0.07	0.02	-0.01	0.00	0.66	0.90	-0.05	0.04
625	63.74	229.31	229.31	0.34	0.52	0.07	0.10	0.32	0.50	-0.01	0.09
645	65.88	436.33	436.33	1.71	2.18	0.34	0.44	-0.17	-0.11	0.28	0.45
655	66.91	14.64	14.64	-1.08	-1.20	-0.22	-0.24	-0.71	-0.75	-0.08	0.01
665	67.93	3.38	3.38	-1.16	-1.29	-0.23	-0.26	0.26	0.42	0.39	0.58
675	68.94	195.12	195.12	0.11	0.24	0.02	0.05	0.61	0.85	0.73	0.99
685	69.92	453.13	453.13	1.82	2.31	0.36	0.46	1.00	1.31	0.85	1.13

695	70.80	162.63	162.63	-0.10	-0.02	-0.02	0.00	0.57	0.79	0.50	0.71
705	71.80	368.71	368.71	1.27	1.64	0.25	0.33	0.84	1.13	0.50	0.71
709	72.19	260.41	260.41	0.55	0.77	0.11	0.15	0.45	0.64	0.69	0.94
715	72.75	286.21	286.21	0.72	0.97	0.14	0.19	0.23	0.38	0.57	0.80
725	73.74	188.98	188.98	0.07	0.19	0.01	0.04	0.74	0.99	0.39	0.58
735	74.73	161.84	161.84	-0.11	-0.02	-0.02	0.00	0.69	0.94	0.29	0.46
745	75.71	515.37	515.37	2.24	2.81	0.45	0.56	0.66	0.90	0.38	0.56
755	76.71	168.62	168.62	-0.06	0.03	-0.01	0.01	-0.22	-0.17	-0.24	-0.19
765	77.71	148.23	148.23	-0.20	-0.13	-0.04	-0.03	-0.09	-0.01	-0.39	-0.37
775	78.72	115.07	115.07	-0.42	-0.40	-0.08	-0.08	-0.32	-0.29	0.10	0.22
795	80.72	227.59	227.59	0.33	0.50	0.07	0.10	-0.45	-0.44	0.16	0.29
801	81.32	45.13	45.13	-0.88	-0.96	-0.18	-0.19	0.19	0.34	-0.02	0.08
805	82.50	57.38	57.38	-0.80	-0.86	-0.16	-0.17	0.44	0.64	0.55	0.77
825	83.50	518.37	518.37	2.26	2.84	0.45	0.57	0.53	0.74	0.95	1.25
835	84.50	158.81	158.81	-0.13	-0.05	-0.03	-0.01	0.43	0.63	0.53	0.74
845	85.49	94.77	94.77	-0.55	-0.56	-0.11	-0.11	0.87	1.16	0.64	0.88
855	86.47	474.71	474.71	1.97	2.49	0.39	0.50	1.10	1.44	1.59	1.24
865	87.45	358.31	358.31	1.20	1.55	0.24	0.31	0.60	0.83	1.14	0.57
875	88.42	200.42	200.42	0.15	0.29	0.03	0.06	1.60	0.47	0.86	0.13
885	89.39	246.15	246.15	0.45	0.65	0.09	0.13	1.46	0.22	0.65	-0.18
895	90.41	809.85		4.19		0.84		1.23		0.42	
905	91.38	137.55	137.55	-0.27	-0.22	-0.05	-0.04	-0.46	-0.45	-0.56	-0.58
915	92.35	140.85	140.85	-0.24	-0.19	-0.05	-0.04	-0.61	-0.64	-0.69	-0.74
925	93.32	46.53	46.53	-0.87	-0.95	-0.17	-0.19	-0.77	-0.83	-0.83	-0.89
935	94.79	69.32	69.32	-0.72	-0.77	-0.14	-0.15	-0.79	-0.85	-0.77	-0.83
945	95.78	69.73	69.73	-0.72	-0.76	-0.14	-0.15	-0.85	-0.92	-0.61	-0.64
955	96.78	38.77	38.77	-0.92	-1.01	-0.18	-0.20	-0.81	-0.88	-0.50	-0.51
965	98.05	41.96	41.96	-0.90	-0.99	-0.18	-0.20	-0.48	-0.48	-0.38	-0.36
975	99.03	86.03	86.03	-0.61	-0.63	-0.12	-0.13	-0.23	-0.18	-0.35	-0.32
985	100.00	188.67	188.67	0.07	0.19	0.01	0.04	-0.13	-0.06	-0.38	-0.36
995	100.95	153.62	153.62	-0.16	-0.09	-0.03	-0.02	-0.41	-0.39	-0.48	-0.47
1005	101.91	130.62	130.62	-0.31	-0.27	-0.06	-0.05	-0.61	-0.63	-0.55	-0.57
1015	102.85	65.76	65.76	-0.74	-0.79	-0.15	-0.16	-0.64	-0.67	-0.21	-0.14
1025	103.80	61.69	61.69	-0.77	-0.83	-0.15	-0.17	-0.57	-0.59	0.24	0.39
1035	104.75	116.77	116.77	-0.40	-0.39	-0.08	-0.08	0.16	0.30	0.30	0.46
1045	105.68	95.76	95.76	-0.54	-0.55	-0.11	-0.11	0.79	1.06	0.37	0.56
1065	107.54	393.92	393.92	1.43	1.84	0.29	0.37	0.81	1.09	0.30	0.47
1071	108.64	401.50	401.50	1.48	1.90	0.30	0.38	0.33	0.50	0.22	0.37
1085	109.20	104.92	104.92	-0.48	-0.48	-0.10	-0.10	-0.47	-0.47	0.05	0.17
1079	110.50	175.15	175.15	-0.02	0.08	0.00	0.02	0.04	0.15	-0.02	0.08
1105	111.43	39.03	39.03	-0.92	-1.01	-0.18	-0.20	0.26	0.41	-0.10	-0.02
1115	112.37	336.07	336.07	1.05	1.37	0.21	0.27	0.29	0.45	0.38	0.56
1125	113.30	273.98	273.98	0.64	0.88	0.13	0.18	-0.21	-0.15	0.07	0.18
1135	114.24	52.72	52.72	-0.83	-0.90	-0.17	-0.18	0.07	0.19	-0.06	0.03

1145	115.17	111.53	111.53	-0.44	-0.43	-0.09	-0.09	0.17	0.32	-0.08	0.01
1155	116.10	400.65	400.65	1.48	1.89	0.30	0.38	0.32	0.50	0.13	0.26
1165	117.04	100.23	100.23	-0.51	-0.52	-0.10	-0.10	-0.47	-0.47	-0.26	-0.21
1175	117.88	179.28	179.28	0.01	0.12	0.00	0.02	-0.10	-0.02	0.52	-0.13
1185	118.81	39.31	39.31	-0.92	-1.01	-0.18	-0.20	-0.26	-0.21	0.30	-0.46
1195	119.84	268.11	268.11	0.60	0.83	0.12	0.17	1.17	0.18	0.36	-0.38
1205	120.78	107.26	107.26	-0.47	-0.46	-0.09	-0.09	0.61	-0.84	0.17	-0.66
1215	121.71	687.15		3.38		0.68		0.55		0.18	
1225	122.64	13.88	13.88	-1.09	-1.21	-0.22	-0.24	-0.69	-0.73	-0.67	-0.70
1235	124.49	81.23	81.23	-0.64	-0.67	-0.13	-0.13	-0.47	-0.47	-0.21	-0.15
1315	131.82	0.28	0.28	-1.18	-1.32	-0.24	-0.26	-0.44	-0.42	-0.49	-0.49
1325	133.02	277.15	277.15	0.66	0.90	0.13	0.18	-0.27	-0.22	-0.42	-0.41
1335	133.95	58.26	58.26	-0.79	-0.85	-0.16	-0.17	-0.65	-0.68	-0.70	-0.74
1345	134.88	75.11	75.11	-0.68	-0.72	-0.14	-0.14	-0.66	-0.70	-0.75	-0.80
1355	136.49	106.79	106.79	-0.47	-0.47	-0.09	-0.09	-0.67	-0.71	-0.56	-0.57
1365	137.41	52.35	52.35	-0.83	-0.90	-0.17	-0.18	-0.86	-0.94	-0.45	-0.44
1375	138.32	69.64	69.64	-0.72	-0.76	-0.14	-0.15	-0.49	-0.49	-0.42	-0.40
1385	139.23	20.08	20.08	-1.05	-1.16	-0.21	-0.23	-0.23	-0.17	-0.38	-0.35
1395	140.56	220.15	220.15	0.28	0.44	0.06	0.09	-0.10	-0.02	-0.26	-0.22
1485	149.62	157.23	157.23	-0.14	-0.06	-0.03	-0.01	-0.32	-0.28	-0.32	-0.28
1495	150.52	102.37	102.37	-0.50	-0.50	-0.10	-0.10	-0.50	-0.50	-0.50	-0.50